ACOUSTIC CHARACTERISTICS OF A LARGE-SCALE AUGMENTOR WING MODEL AT FORWARD SPEED

by Michael D. Falarski and David G. Koenig

Ames Research Center

and

U.S. Army Air Mobility R&D Laboratory

Moffett Field, Calif. 94035

1. Report No. NASA TM X–2940	2. Government Accession No.	3. Recipient's Catalog No.
4. Title and Subtitle ACOUSTIC CHARACTERISTICS OF A LARGE-SCALE AUGMENTOR WING MODEL AT FORWARD SPEED		5. Report Date November 1973
		6. Performing Organization Code
7. Author(s) Michael D. Falarski and David G. Koenig		8. Performing Organization Report No. A-4964
		10. Work Unit No. 760-62-01
9. Performing Organization Name and Address Ames Research Center and U.S. Army Air Mobility R&D Laboratory Moffett Field, Calif. 94035		11. Contract or Grant No.
		13. Type of Report and Period Covered Technical Memorandum
12. Sponsoring Agency Name and Address National Aeronautics and Space Administration Washington, D.C. 20546		14. Sponsoring Agency Code
15. Supplementary Notes		

16. Abstract

The augmentor wing concept is being studied as one means of attaining short takeoff and landing (STOL) performance in turbofan powered aircraft. Because of the stringent noise requirements for STOL operation, the acoustics of the augmentor wing are undergoing extensive research. This paper presents the results of a wind tunnel investigation of a large-scale swept augmentor model at forward speed. The augmentor was not acoustically treated, although the compressor supplying the high pressure primary air was treated to allow the measurement of only the augmentor noise.

Installing the augmentor flap and shroud on the slot primary nozzle caused the acoustic dependence on jet velocity to change from eighth power to sixth power.

Deflecting the augmentor at constant power increased the perceived noise level in the forward quadrant.

The effect of airspeed was small. A small aft shift in perceived noise directivity was experienced with no significant change in sound power.

Sealing the lower augmentor slot at a flap deflection of 70° reduced the perceived noise level in the aft quadrant. The seal prevented noise from propagating through the slot.

17. Key Words (Suggested by Author(s)) Noise STOL STOL Noise	18. Distribution Statement Unclassified — Unlimited		
19. Security Classif. (of this report) Unclassified	20. Security Classif. (of this page) Unclassified	21. No. of Pages 42	22. Price* Domestic, $3.00 Foreign, $5.50

NOTATIONS

OASPL   overall sound pressure level, dB ref. 2×10^{-5} N/m^2 (0.0002 microbar)

P_r augmentor primary jet pressure ratio

PNL   perceived noise level, PNdB

PWL   sound power level, dB ref. 10^{-12} W

q   free-stream dynamic pressure, $\dfrac{\text{N}}{\text{sq m}}$ (lb/sq ft)

SPL   sound pressure level, dB ref. 2×10^{-5} N/m^2 (0.0002 microbar)

V_∞ free-stream velocity, knots

δ_f flap deflection, deg

ACOUSTIC CHARACTERISTICS OF A LARGE-SCALE

AUGMENTOR WING MODEL AT FORWARD SPEED

Michael D. Falarski and David G. Koenig

Ames Research Center

and

U.S. Army Air Mobility Research and Development Laboratory

SUMMARY

The augmentor wing concept is being studied as one means of attaining short takeoff and landing (STOL) performance in turbofan powered aircraft. Because of the stringent noise requirements for STOL operation, the acoustics of the augmentor wing are undergoing extensive research. This paper presents the results of a wind tunnel investigation of a large-scale swept augmentor model at forward speed. The augmentor was not acoustically treated, although the compressor supplying the high pressure primary air was treated to allow the measurement of only the augmentor noise.

Installing the augmentor flap and shroud on the slot primary nozzle caused the acoustic dependence on jet velocity to change from eighth power to sixth power.

Deflecting the augmentor at constant power increased the perceived noise level in the forward quadrant.

The effect of airspeed was small. A small aft shift in perceived noise directivity was experienced with no significant change in sound power.

Sealing the lower augmentor slot at a flap deflection of 70° reduced the perceived noise level in the aft quadrant. The seal prevented noise from propagating through the slot.

INTRODUCTION

The augmentor wing concept is being studied as one means of attaining STOL performance in turbofan powered aircraft. As a STOL aircraft, it will be operating out of STOL ports in densely populated areas. This location will require its noise levels to be substantially lower than today's conventional takeoff and landing (CTOL) aircraft. Augmentor wing acoustic characteristics and noise suppression techniques are therefore undergoing extensive study. The results of one investigation using small-scale models at static conditions ($V_\infty = 0$) are documented in reference 1. This paper presents the results of a wind tunnel investigation of the acoustic characteristics of a large-scale swept augmentor wing model at forward speed. The aerodynamic characteristics were

also investigated and are reported in references 2 and 3. The investigations were performed in the Ames 40- by 80-Foot (12.2- by 24.4-m) Wind Tunnel.

This research program was undertaken in cooperation with the Defence Research Board of Canada and DeHavilland Aircraft of Canada, Ltd.

MODEL AND APPARATUS

The model is shown installed in the wind tunnel in figure 1(a) and on the static test stand in figure 1(b). The basic geometry of the model is shown in figure 2(a—e) and model reference dimensions and airfoil coordinates are listed in tables 1 through 3.

Augmentor Flap

The geometry of the augmentor flap is shown in figure 2(c). The augmentor is an ejector system partly consisting of a trailing edge primary nozzle (fig. 2(d)) through which high pressure air is delivered; a lower flap, upper shroud, and intake door form the rest of the augmentor. The secondary air is entrained from the wing upper surface, a slot between the intake door and shroud, and a lower slot between the wing lower surface and flap. The mixed jet is ejected downward between the flap and shroud. The angle of the intake door was optimized for each flap deflection.

The ducting for the primary air and aileron boundary layer control (BLC) is shown in figure 2(b). The ducting was designed to maintain a constant duct Mach number of 0.36 at a pressure ratio of 1.8.

Aileron BLC

The geometry of the aileron BLC is shown in figure 2(e). The system was fed through an extension of the augmentor primary air duct and was therefore coupled with the augmentor. The BLC was approximately 5 percent of the total compressor output. The ailerons were drooped symmetrically to 30° for the acoustic investigation.

Turbo-Compressor

The high pressure primary air for the augmentor and aileron BLC was provided by the turbo-compressor unit shown in figure 3. It consists of a J-85 pneumatically coupled to two modified Viper engines. The exhaust gas of the J-85 is split and ducted to the turbine section of the Vipers. The output of the Viper compressor is then piped into the wing. The residual J-85 exhaust is ducted out the aft end of the fuselage.

2

Turbo-Compressor Acoustic Treatment

For the acoustic investigation, the turbocompressor inlets and J-85 residual gas tailpipes were acoustically treated to suppress the fan machinery noise and residual gas jet noise. The suppressors are shown installed on the model in figure 1(a). The photograph of the model in the static test support shows the model with the suppressors removed. A comparison of the acoustic frequency spectrum with and without the suppressor is shown in figure 4. The high frequency fan machinery pure tones and broadband noise were attenuated by the inlet suppressors. The tailpipe suppressor shifted the residual gas jet noise from the 100—400 Hz range to the 12.5—50 Hz range by reducing the mixed velocity and increasing the effective diameter. Thus, the turbocompressor acoustic treatment separated the frequency of the residual jet noise and the augmentor noise so that the noise of the augmentor could be extracted from the data.

TESTS

Static Tests

The acoustic characteristics of the model were investigated in the free-field as well as in the wind tunnel. The model was mounted on the support system shown in figure 1(b). The microphone arrangements for underwing and sideline measurements are presented in figure 5. The noise measurements were made with Bruel and Kjaer 1.27cm (1/2 in.) diameter, type 4133, condenser microphones and recorded on Ampex F1300A multi-channel tape recorders. The underwing microphones were equipped with aerodynamic-shaped, omnidirectional nose cones. The sideline microphones were equipped with porous, polyurethane, sponge windscreens.

The noise of the model was measured at primary nozzle pressure ratios (P_r) of 1.0 to 1.9 for flap deflections of 30°, 40°, 60°, and 70°.

Wind Tunnel

The effects of forward speed on the acoustics of the model were measured in the wind tunnel. The test procedure consisted of varying the primary nozzle pressure ratio at a constant dynamic pressure. The pressure ratio was varied from 0 to 1.9 while forward speed was varied from 0 to 77 knots. Noise data were recorded at flap deflections of 30°, 40°, 60°, and 70°. A series of tests was also made at $\delta_f = 70°$ with the lower augmentor slot sealed as shown in figure 6. The underwing microphones and microphone arrangement used in the wind tunnel were the same as described for the static underwing noise measurement.

DATA REDUCTION

Reverberation Corrections

The acoustic environment of the wind tunnel has been investigated with several acoustic sources. From these studies various techniques have been derived to allow the prediction of free-field noise levels from wind tunnel acoustic measurements. These techniques and the comparison of wind tunnel and flight data are reported in references 4 and 5.

The raw noise data were reduced to a one-third octave band frequency spectrum with a Bruel and Kjaer Real Time Spectral Analyzer. The wind tunnel spectra were corrected for test section reverberation. The corrections were derived from the difference between the spectra of the static and wind tunnel test results for the takeoff ($\delta_f = 40°$) configuration at several pressure ratios. This technique assumes the static results to be free-field; therefore, the difference is caused only by reverberation. Typical reverberation corrections for two microphones are shown in figure 7. The corrections were independent of pressure ratio; when applied to wind tunnel results at other flap deflections, they produced very good agreement with the static results.

Background Noise Level

The operation of the wind tunnel and the flow of air over the microphones create a background noise floor. To study the acoustics of a source in this environment, the sound pressure levels of the source must be of sufficient magnitude to be distinguishable from the background. A comparison of the augmentor wing model and the wind tunnel background is presented in figure 8. The model noise is at least 10 dB above the background noise floor, thus eliminating any need for correction of the model data.

Calculation of Sound Power Level

Investigations of the acoustic environment in the wind tunnel test section inlet and diffuser have shown that the acoustic energy flows out of the test section and is fairly diffuse in these areas. The sound power generated by the model was estimated using a simple technique derived from these results (ref. 4). The technique requires only a single measurement of the sound pressure level in the wind tunnel inlet and diffuser.

Scaling and Presentation

The data were projected to 152.5 m (500 ft) and scaled to a 150 passenger, 91,000 kg (200,000 lb) aircraft, assuming a nozzle pressure ratio of 1.8 and 80 percent of the installed thrust directed into the wing. The scaling technique has been described in reference 6. The model values of pressure ratio and total temperature were assumed to be equivalent to full-scale. The scale factor, which is the square root of the ratio of the full-scale nozzle area to the model nozzle area, was 6.6. The projection to 152.5 m (500 ft) was accomplished using the standard Society of Automotive Engineers procedures in reference 7.

The data are presented as one-third octave band frequency spectra and perceived noise level directivity curves. The directivity curves were developed by plotting PNL versus the sideline or underwing angles shown in figure 5(b). The underwing microphones were in a plane 35° below the plane of the wing.

RESULTS AND DISCUSSION

The acoustic energy radiated by the efflux of a slot nozzle varies with the eighth power of the jet velocity, as can be seen in figure 9. This eighth power dependence agrees with jet noise theory and experiments. When the augmentor flap and shroud assembly were installed, the SPL varied with the sixth power of the jet velocity, indicating a modification of the acoustic generation mechanism. This sixth power dependence indicates the dominant acoustic source has become the fluctuating loads on the augmentor created by the interaction of the flow turbulence with the augmentor. It has also been shown in references 1 and 8 that installing the augmentor reduced the peak OASPL for takeoff flap configurations. The augmentor apparently reduced the jet noise because of the reduced turbulence and lower velocities created by the entrainment of secondary air into the augmentor.

Effect of Augmentor Flap Deflection, $V_\infty = 0$ knots

The underwing and sideline perceived noise level directivity patterns of the various augmentor flap deflections are compared in figures 10 and 11. Neither the landing configurations ($\delta_f = 60°$ or 70°) nor the takeoff configurations ($\delta_f = 30°$ or 40°) are highly directional. The PNL's in the forward quadrant are higher for the landing configurations. The difference in underwing noise was 4 PNdB at a pressure ratio of 1.83. These increases in PNL are the result of broadband modifications in the augmentor frequency spectra as shown in figure 12.

The variation in noise with flap deflection can either be attributed to a redistribution of the same overall acoustic enegy, or to a change in the overall energy, or both. The total acoustic energy of a source is indicated by the sound power level (PWL). The effect of flap deflection on the PWL of the augmentor wing is presented in figure 13. It can be seen that the PWL, like the PNL, is greater for the landing flap; therefore, the total acoustic energy has increased. Because this energy is probably generated by fluctuating loads from turbulent flow, flap deflection must increase the flow turbulence and/or increase the interaction of the flow with the augmentor surfaces. This acoustic energy is probably created by the increased flow turning inside the augmentor at high flap deflections.

These results, of course, do not necessarily imply that during approach the augmentor will be noisier. In fact, it will probably be quieter because of a lower throttle setting for approach.

Effect of Forward Speed

The effect of forward speed on the acoustics of the augmentor wing was small. There was a small aft shift in directivity, as can be seen in figures 14—18, with the high flap deflections having the greatest shift. The peak PNL decreased slightly with forward speed for the takeoff configuration, while the opposite happened for the landing flaps. In both cases the change was approximately 1 PNdB for the range of forward speeds investigated. The shift in directivity produced little change in sound power, denoting an insignificant change in the total acoustic energy (see fig. 19). The frequency spectra in figure 20 show that the PNL directivity shift was produced by broadband variations in the frequency. These small alterations in acoustics may be the result of turbulence modification by the free-stream inlet momentum.

Effect of Sealing the Lower Augmentor Slot

The lower slot between the main wing and augmentor flap allows air to be entrained into the augmentor from the wing undersurface. This slot is a possible source of noise. For this reason a series of tests was made with the slot sealed at $\delta_f = 70°$ as shown in figure 6. The effect of this seal on the perceived noise is presented in figure 21. The primary effect of the seal was to reduce the PNL in the aft quadrant. The maximum reduction was 3 PNdB at $V_\infty = 0$ knots and 2 PNdB at $V_\infty = 77$ knots. The reduction in PNL results from a decrease in the high frequency bands of the spectra as shown in figure 22. These reductions could be derived from two sources. The shielding of the seal prevents noise from propagating through the slot. It is also possible the seal could eliminate a source of noise by preventing flow through the slot which interacts with the augmentor surfaces. The prevention of noise propagation through the slot is most likely the cause for the majority of the noise reduction.

CONCLUDING REMARKS

The acoustic energy radiated by the augmentor slot primary nozzle varies with the eighth power of the jet velocity. When the augmentor flap and shroud are installed, the acoustic mechanism is modified such that the noise varies with the sixth power of the jet velocity. The dominant acoustic source has become the interaction of the turbulent flow with the augmentor.

Deflecting the flap at a constant pressure ratio increased the PNL in the front quadrant and increased the total sound power. This observation indicates that the increse in flap deflection not only redistributes the acoustic energy but also increases the overall acoustic energy generated. This effect probably results from an increase in turbulence and the interaction of this turbulence with the augmentor surfaces resulting from the higher primary air turning inside the augmentor.

The effect of airspeed was small. There was a slight aft shift in PNL directivity, with no significant change in total sound power.

The PNL was reduced in the aft quadrant by sealing the augmentor lower slot. The seal prevented noise generated in the augmentor from propagating out of the slot.

These results are for an augmentor that was not acoustically treated. The effect of forward speed will probably be greater with a treated model because of the reduced augmentor velocities and the greater dominance of the noise generated at the augmentor exit. The variation with flap deflection will also change because the treated augmentor will probably require less turning of the primary air.

Ames Research Center
National Aeronautics and Space Administration
Moffett Field, California 94035, June 1973

REFERENCES

1. O'Keefe, Jack V.; and Kelly, George S.: Design Integration and Noise Studies for Jet STOL Aircraft. NASA CR-114471, 1972.

2. Falarski, Michael D.; and Koenig, David G.: Longitudinal and Lateral Stability and Control Characteristics of a Large-Scale Model with a Swept Wing and Augmented Jet Flap. NASA TM X-62,145, 1972.

3. Falarski, Michael D.; and Koenig, David G.: Longitudinal Aerodynamic Characteristics of a Large-Scale Model with a Swept Wing and an Augmented Jet Flap in Ground Effect. NASA TM X-62,174, 1972

4. Bies, David A.: Investigation of the Feasibility of Making Model Acoustic Measurements in the NASA Ames 40- by 80-Foot Wind Tunnel. NASA CR-114,352, 1971.

5. Falarski, Michael D.; Koenig, David G.; and Soderman, Paul T.: Aspects of Investigating STOL Noise Using Large-Scale Wind Tunnel Models. NASA TM X-62,164, 1972.

6. Morgan, Walter V.; Sutherland, L. C.; and Young, Kenneth J.: The Use of Acoustic Scale Models for Investigating Near Field Noise of Jet and Rocket Engines. WADD TR 61-178, 1961.

7. Anon.: Standard Values of Atmospheric Absorption as a Function of Temperature and Humidity for Use in Evaluating Aircraft Flyover Noise. SAE ARP 866, 1964.

8. Gibson, Fredrick W.: Noise Measurements of Model Jet-Augmented Lift Systems. NASA TN D-6710, 1972.

TABLE 1.—WING REFERENCE DIMENSIONS

Wing area, sq m (sq ft)	21.36	(230.0)	
Aspect ratio	8.0		
Span, m (ft)	13.08	(42.895)	
Taper ratio	0.30		
Sweep at ¼ chord, deg	27.5		
Airfoil section	RAE 104		
Root chord, m (ft)	2.515	(8.25)	
Tip chord, m (ft)	0.755	(2.475)	
Root thickness, percent	12½		
Tip thickness, percent	10½		
Augmentor span limits, inner, m (ft) (percent)	1.111	(3.645)	(12.34)
Augmentor span limits, outer, m (ft) (percent)	4.575	(15.01)	(70.0)
Wing area spanned by one augmentor, sq m (sq ft)	6.75	(72.62)	
Wing area spanned by one aileron, sq m (sq ft)	1.997	(21.50)	
Wing area spanned by fuselage, sq m (sq ft)	3.88	(41.77)	
Flap hinge axis, percent chord	68.543		
Aileron hinge axis, percent chord	68.0		
Incidence, camber, twist	0		
Mean aerodynamic chord, m (ft)	1.793	(5.880)	

Note: All chords are measured in streamwise direction.

TABLE 2.—TAIL REFERENCE DIMENSIONS

Horizontal Tail		
Gross area, sq m (sq ft)	5.58	(60.0)
Aspect ratio	4.5	
Span, m (ft)	5.005	(16.432)
Taper ratio	0.40	
Sweep at ¼ chord, deg	25	
Airfoil section	RAE 104 with modified leading edge	
Thickness/chord ratio, percent	10	
Root chord, m (ft)	1.591	(5.22)
Tip chord, m (ft)	0.635	(2.082)
Elevator hinge axis	see figure 3(c)	
Elevator travel, deg	±30	
Tailplane incidence, deg	±12	
Tailplane arm, m (ft)	6.804	(22.32)
Tailplane volume coefficient	0.990	
Mean aerodynamic chord, m (ft)	1.114	(3.654)
Vertical Fin		
Fin arm, m (ft)	5.361	(17.603)
Fin volume coefficient	0.07476	

TABLE 3.—COORDINATES OF ROYAL AERONAUTIC ESTABLISHMENT 104 AIRFOIL (t/c max. = 0.10)

x/c	y/c(100)	x/c	y/c(100)
0	0	0.35	4.9300
0.001	0.3441	.35	4.9488
.002	.4863	.38	4.9775
.003	.5953	.4	4.9946
.004	.6870	.42	5.0000
.005	.7676	.44	4.9937
.006	.8404	.45	4.9862
.007	.9072	.46	4.9756
.0075	.9387	.48	4.9454
.008	.9692	.5	4.9027
.009	1.0274	.52	4.8468
.01	1.0824	.54	4.7769
.012	1.1842	.55	4.7363
.0125	1.2083	.56	4.6917
.014	1.2776	.58	4.5802
.016	1.3642	.6	4.4650
.018	1.4452	.62	4.3113
.02	1.5215	.64	4.1370
.025	1.6960	.65	4.0438
.03	1.8522	.66	3.9473
.035	1.9945	.68	3.7452
.04	2.1256	.7	3.5331
.05	2.3617	.72	3.3128
.06	2.5709	.74	3.0861
.07	2.7592	.75	2.9708
.075	2.8468	.76	2.8545
.08	2.9307	.78	2.6103
.09	3.0881	.8	2.3819
.1	3.2336	.82	2.1437
.12	3.4945	.84	1.9055
.14	3.7222	.85	1.7864
.15	3.8254	.86	1.6673
.16	3.9224	.88	1.4202
.18	4.0992	.9	1.1910
.2	4.2556	.92	0.9528
.22	4.3936	.925	.8932
.24	4.5149	.94	.7146
.25	4.5697	.95	.5955
.26	4.6208	.96	.4764
.28	4.7124	.975	.2977
.3	4.7905	.98	.2382
.32	4.8556	.9875	.1489
.34	4.9082	1.0	0

(a) Model installed in wind tunnel with noise suppressors.

Figure 1.— Augmentor wing model installations.

(b)   Model without noise suppressors installed on static test stand.

Figure 1.— Concluded.

(a) Geometric details of augmentor wing model.
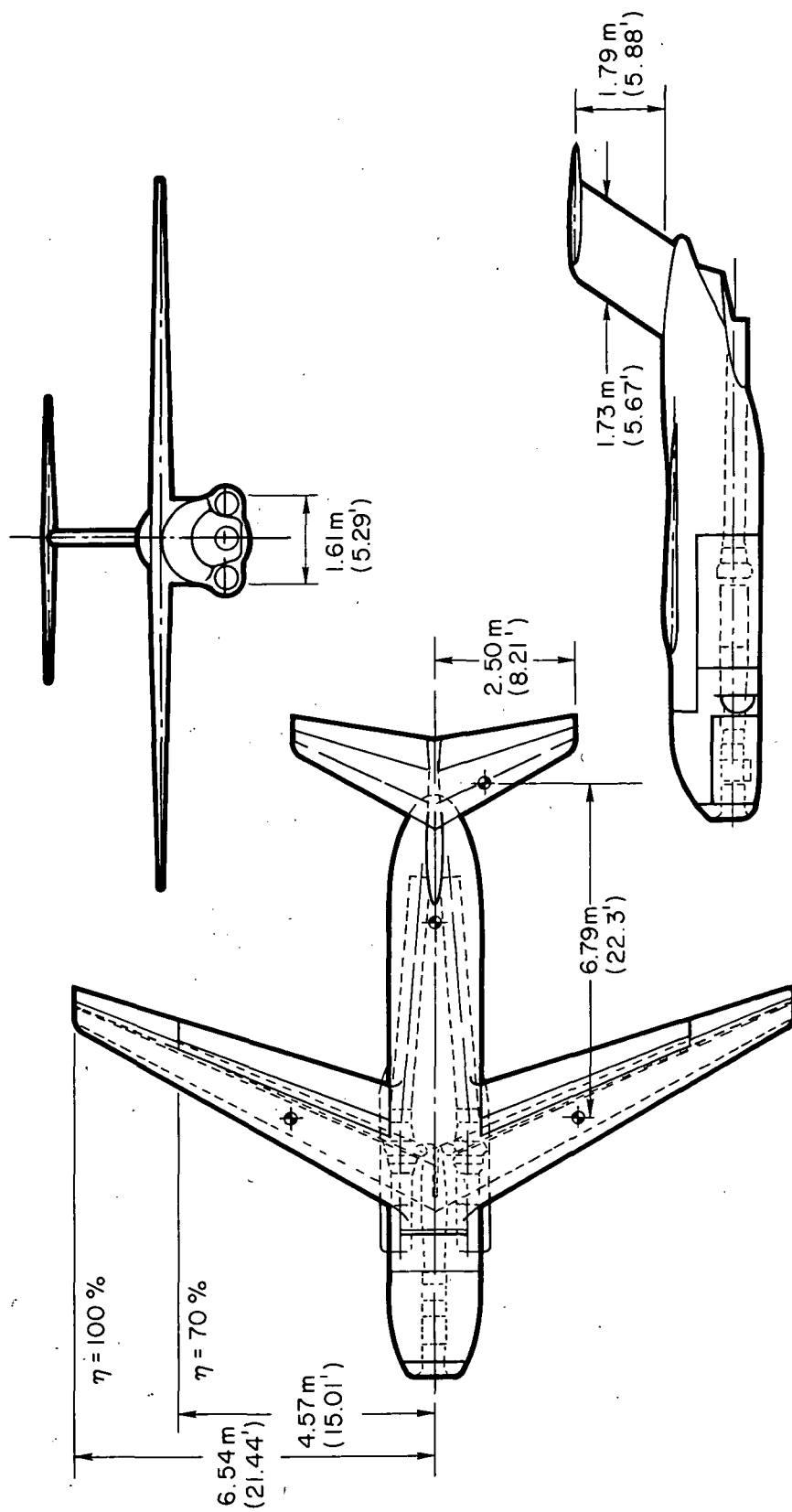
Figure 2.— Geometric details of augmentor wing model.

13
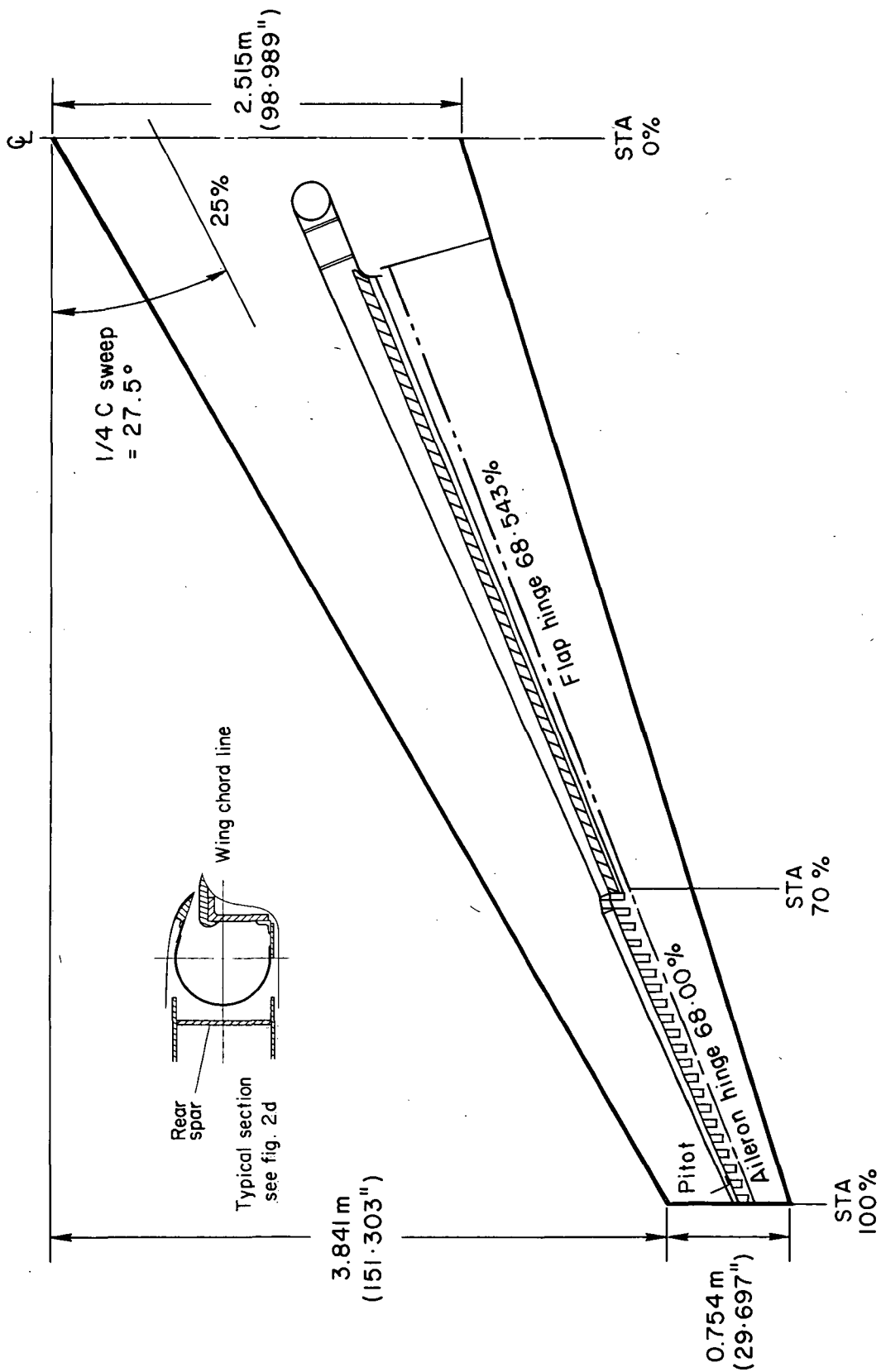
(b) Wing platform geometry and ducting.

Figure 2.— Continued.

(c) Augmentor geometry.
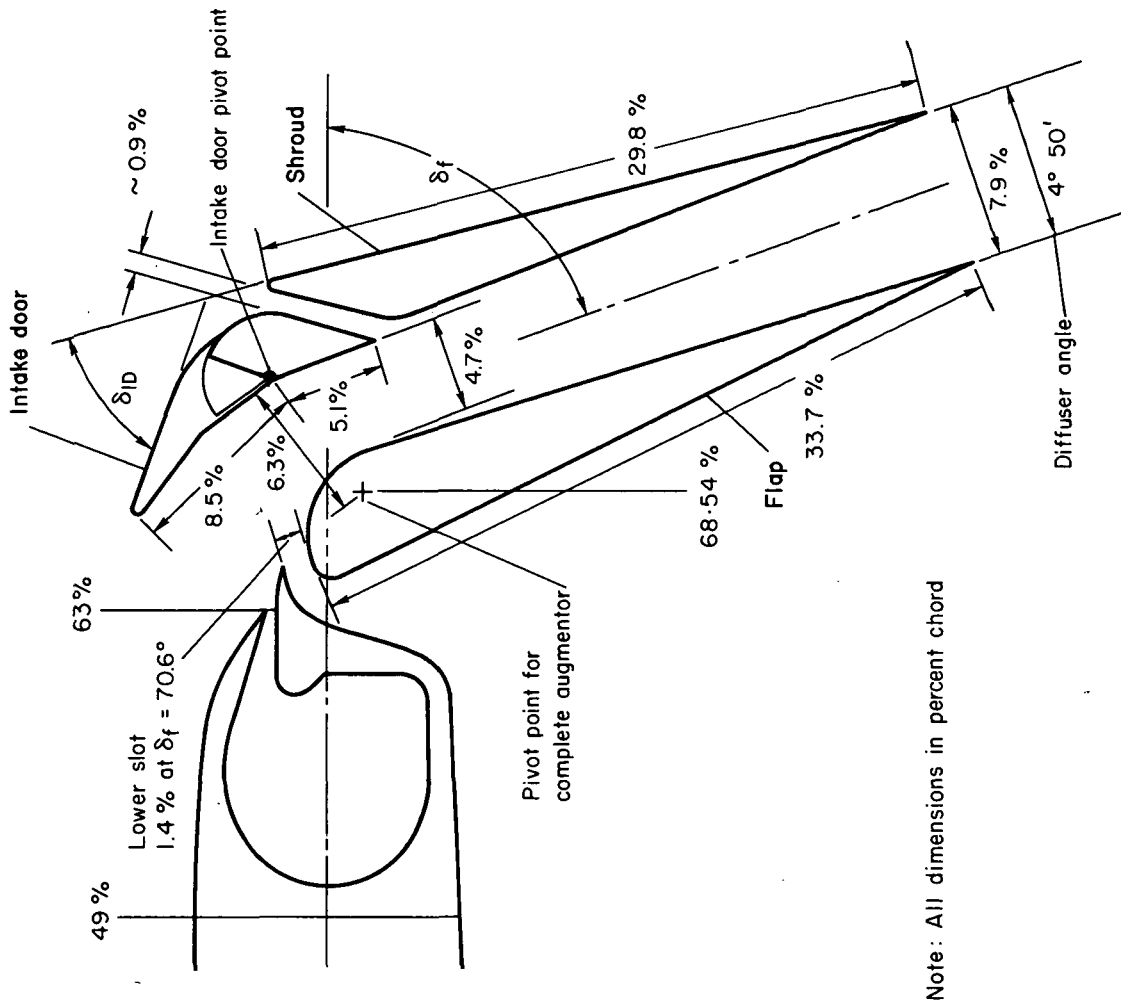
Figure 2.— Continued.

Note: All dimensions in percent chord

15

63% Chord

45°

Nozzle vane

0.35% Chord

A

A

17.5°

22°

Nozzle exit plane

Section A-A
Typical nozzle vane
Pitch = 10 × nozzle thickness
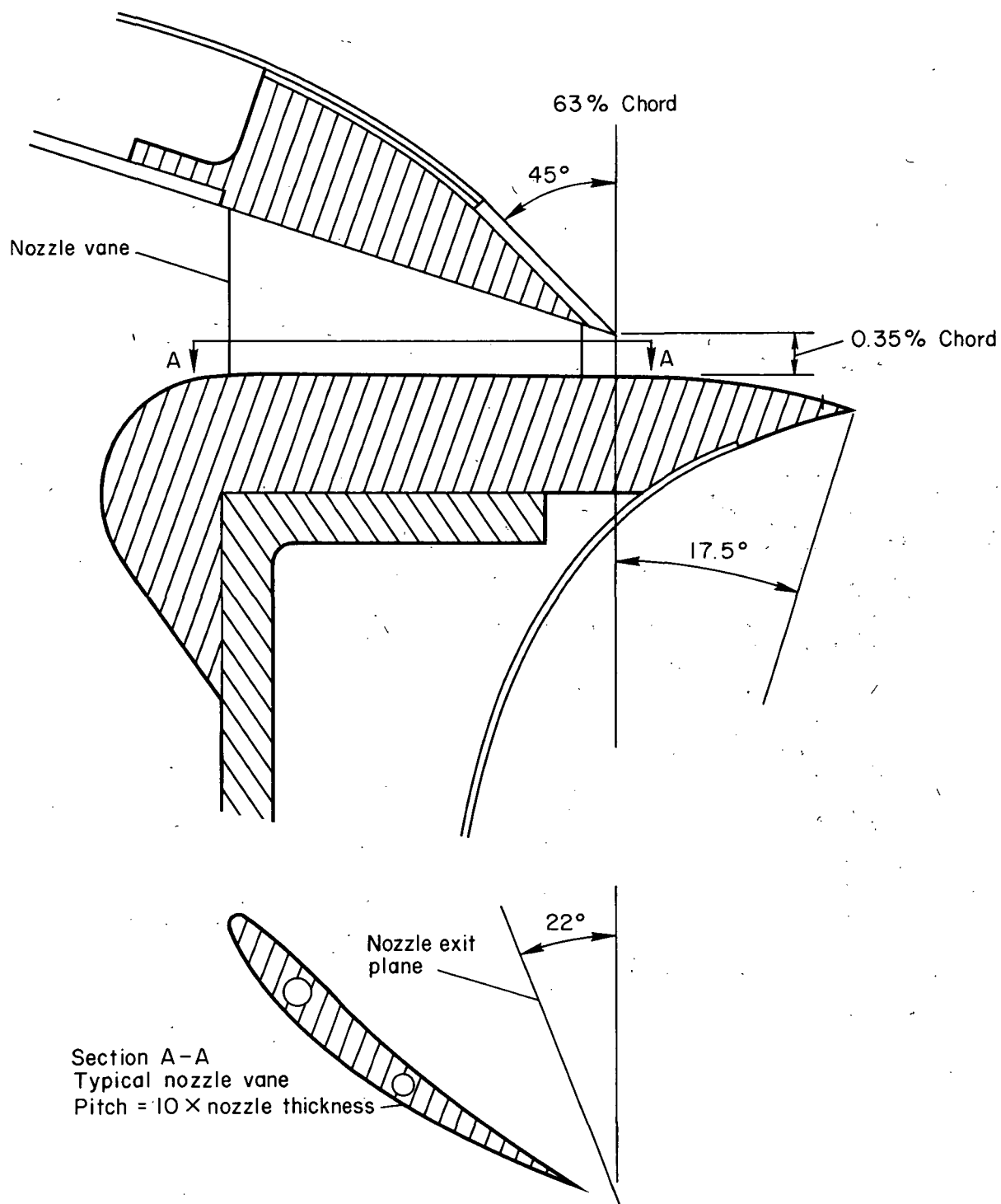
(d)   Augmentor slot primary nozzle details.

Figure 2.— Continued.

STA 70%

STA 100%

STA 63.7 %

BLC nozzle

Pivot point
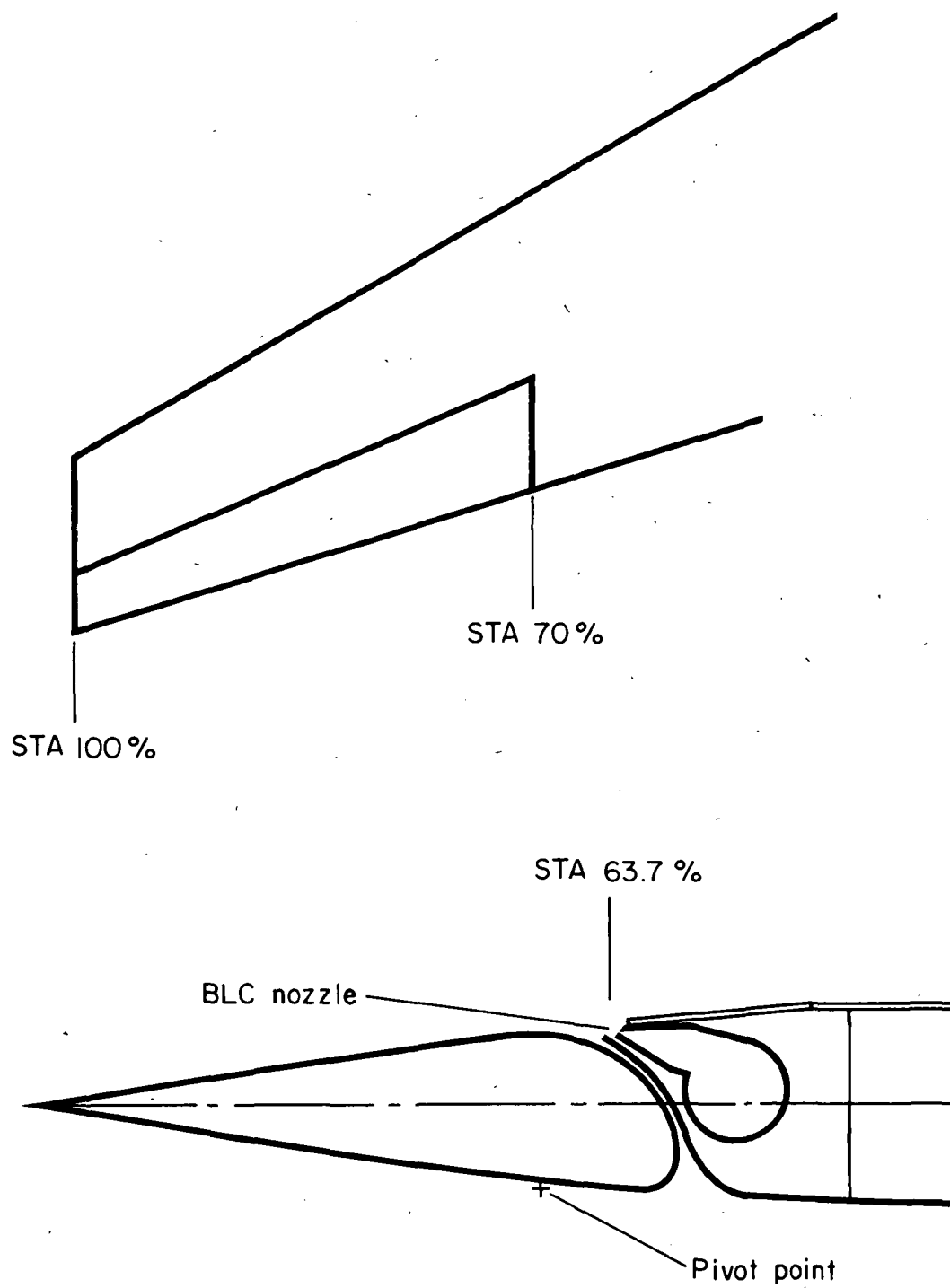
(e)   Aileron BLC geometry.

Figure 2.— Concluded.

Residual hot gas exhaust

J-85 gas generator (compressor bleed for fuselage BLC)

Viper 8 load compressors

Model ₵

Airflow

Air supplies to wing jet augmentors and aileron BLC

Model ₵
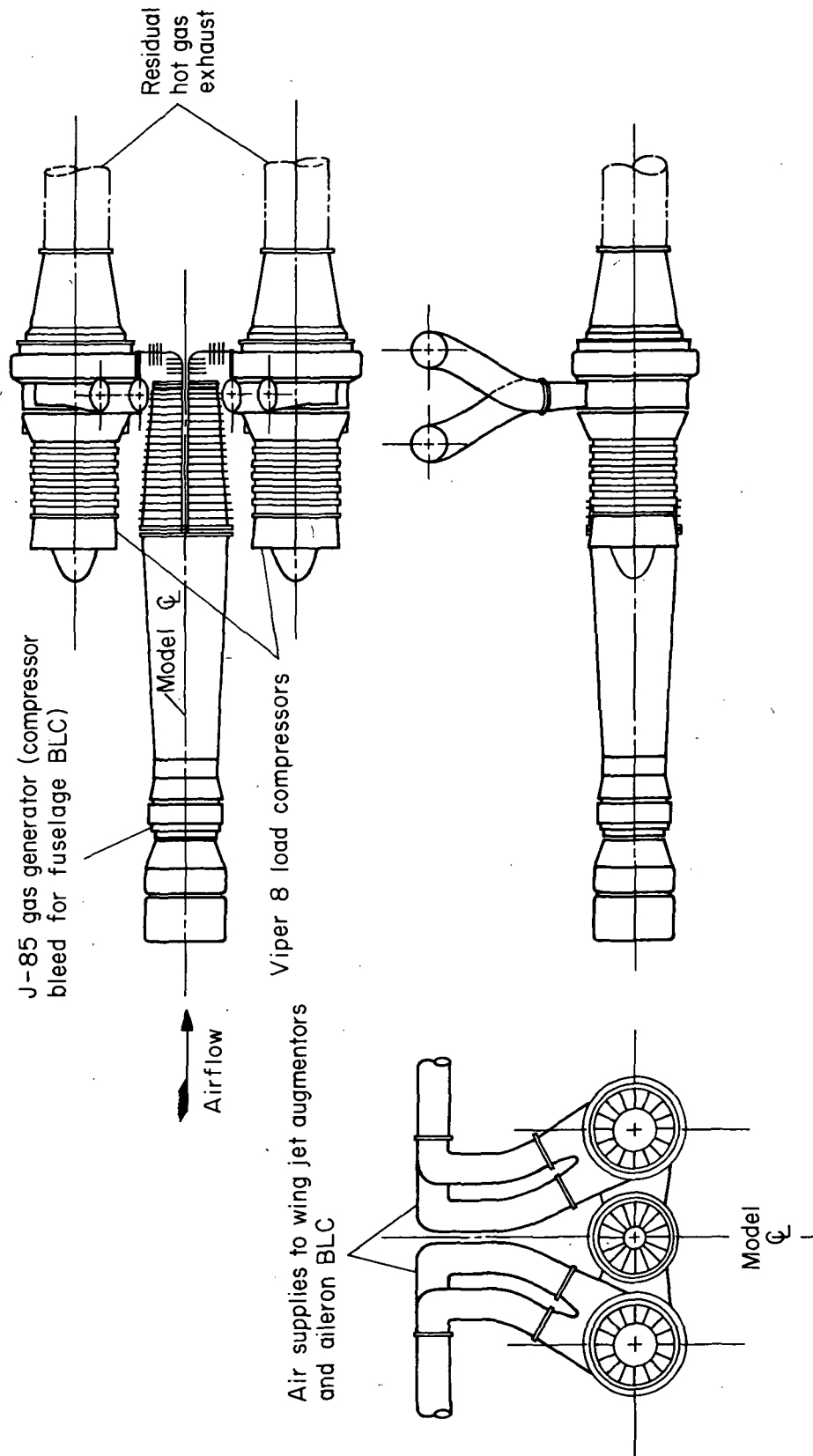
Figure 3.— Augmentor air compressor system.
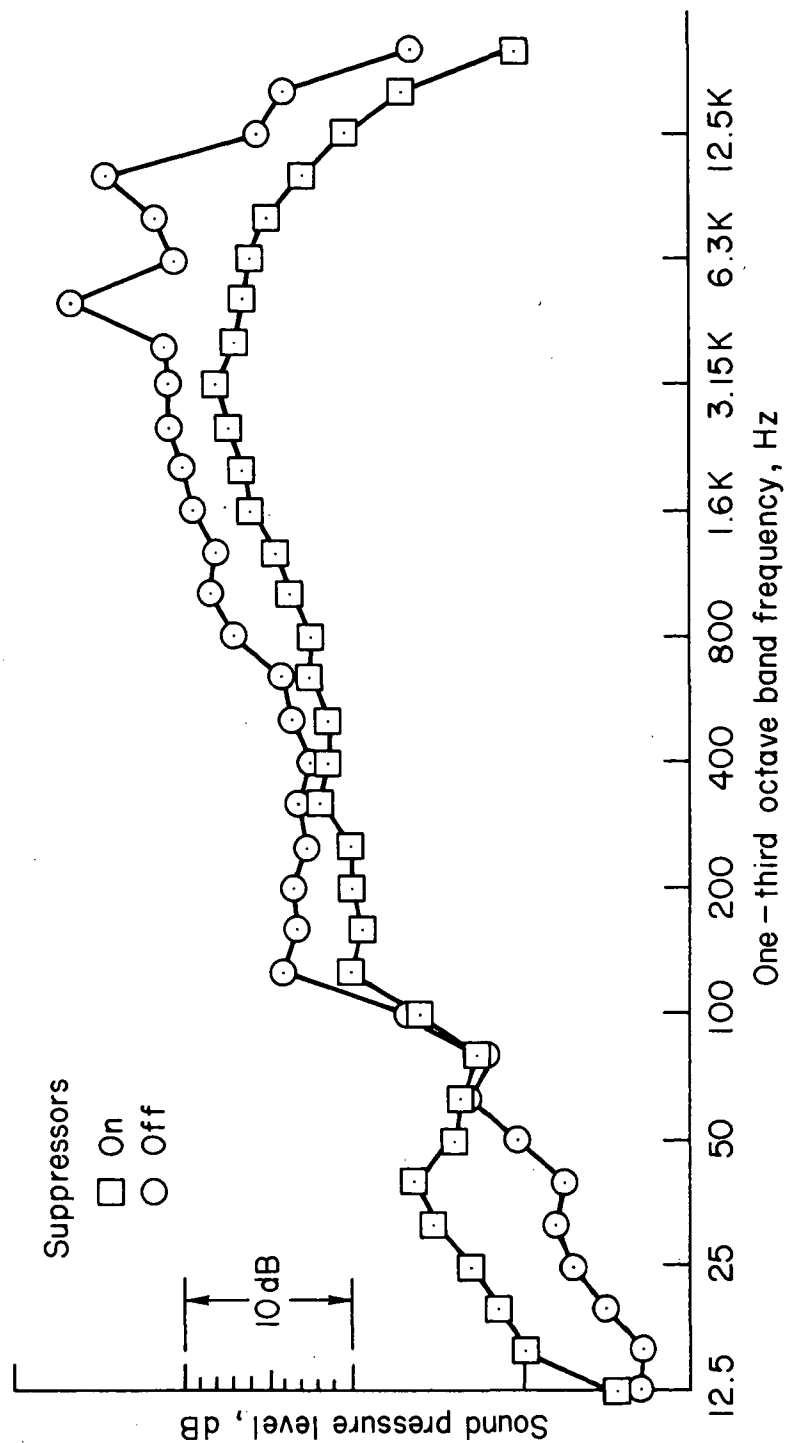
Figure 4.— Suppression of compressor inlet noise with acoustically lined inlets.
$\delta_f = 40°$; $P_I = 1.83$; 70° sideline azimuth.

Sideline microphone azimuth = 70°

1.27 cm (1/2 in.) Microphone
5.18 m (17 ft) Above ground

22.9 m (75 ft)

Model mounted on static test stand
6.4 m (21 ft) Above ground

10°
30°
50°
90°
110°
130°
150°
170°
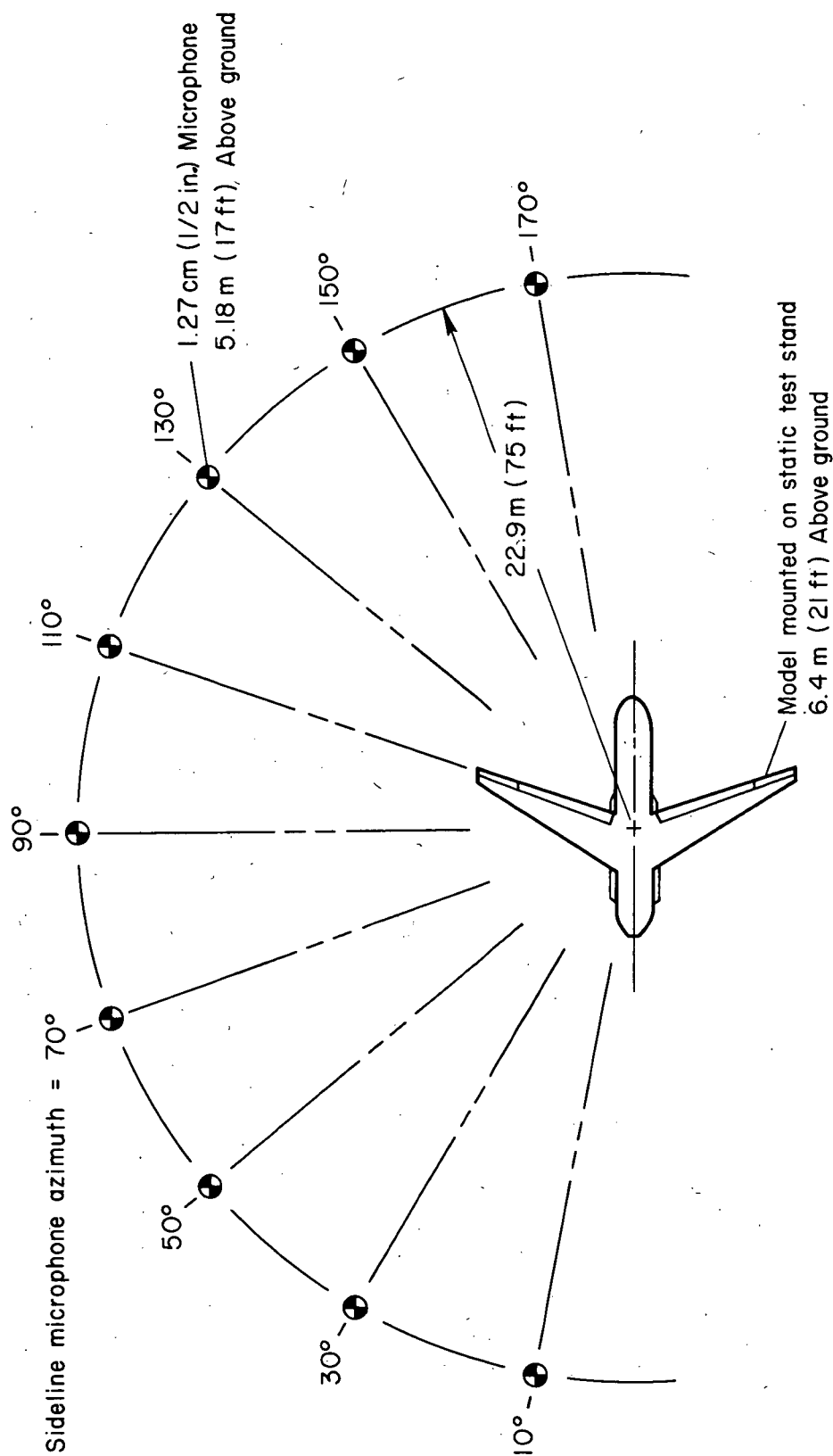
(a)   Sideline microphone arrangement for static test.

Figure 5.— Microphone locations.

1.27 cm (1/2 in.) Condenser microphone with aerodynamic nose cone

Acoustic center

6.54 m (21.45 ft)

Acoustic center

Underwing angle = 43°

54°
76°
97°
116°
134°
143°
152°

6.16 m (20.2 ft)

1.83 m (6 ft)
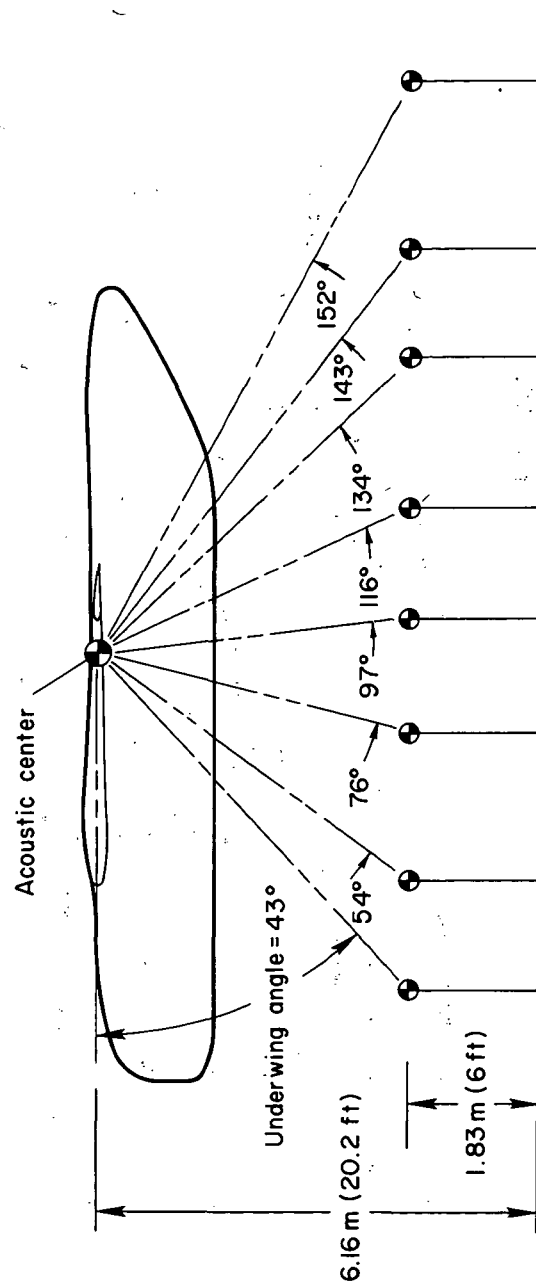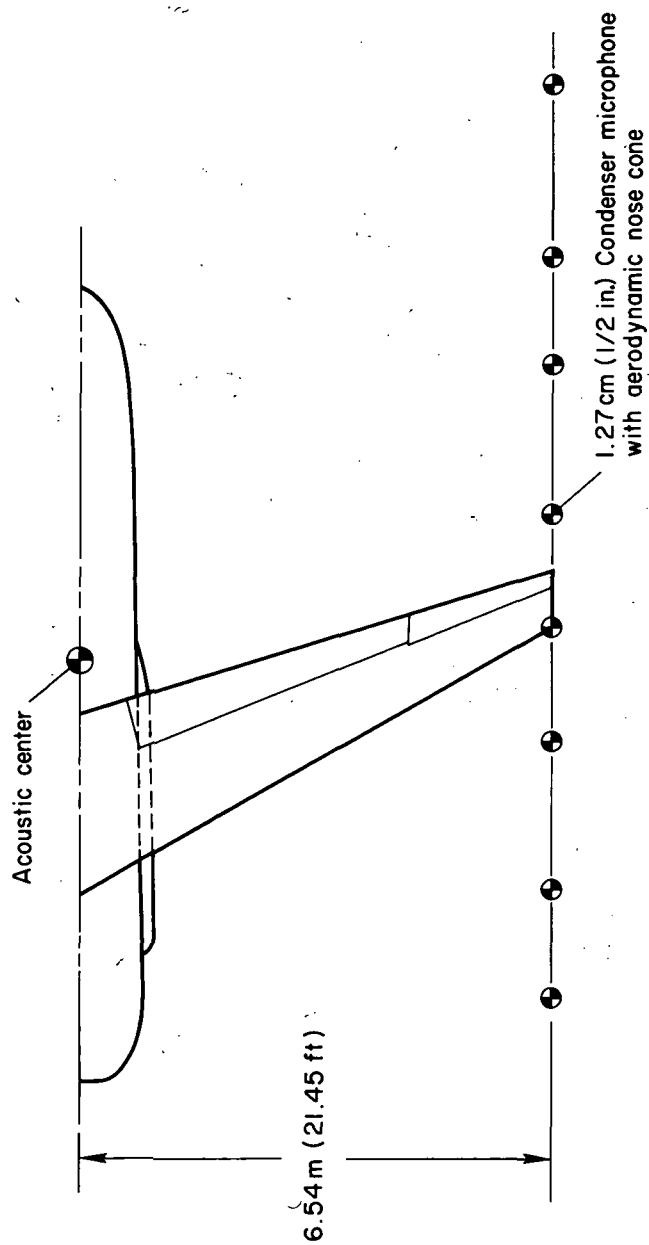
(b) Underwing microphone arrangement.

Figure 5.— Concluded.
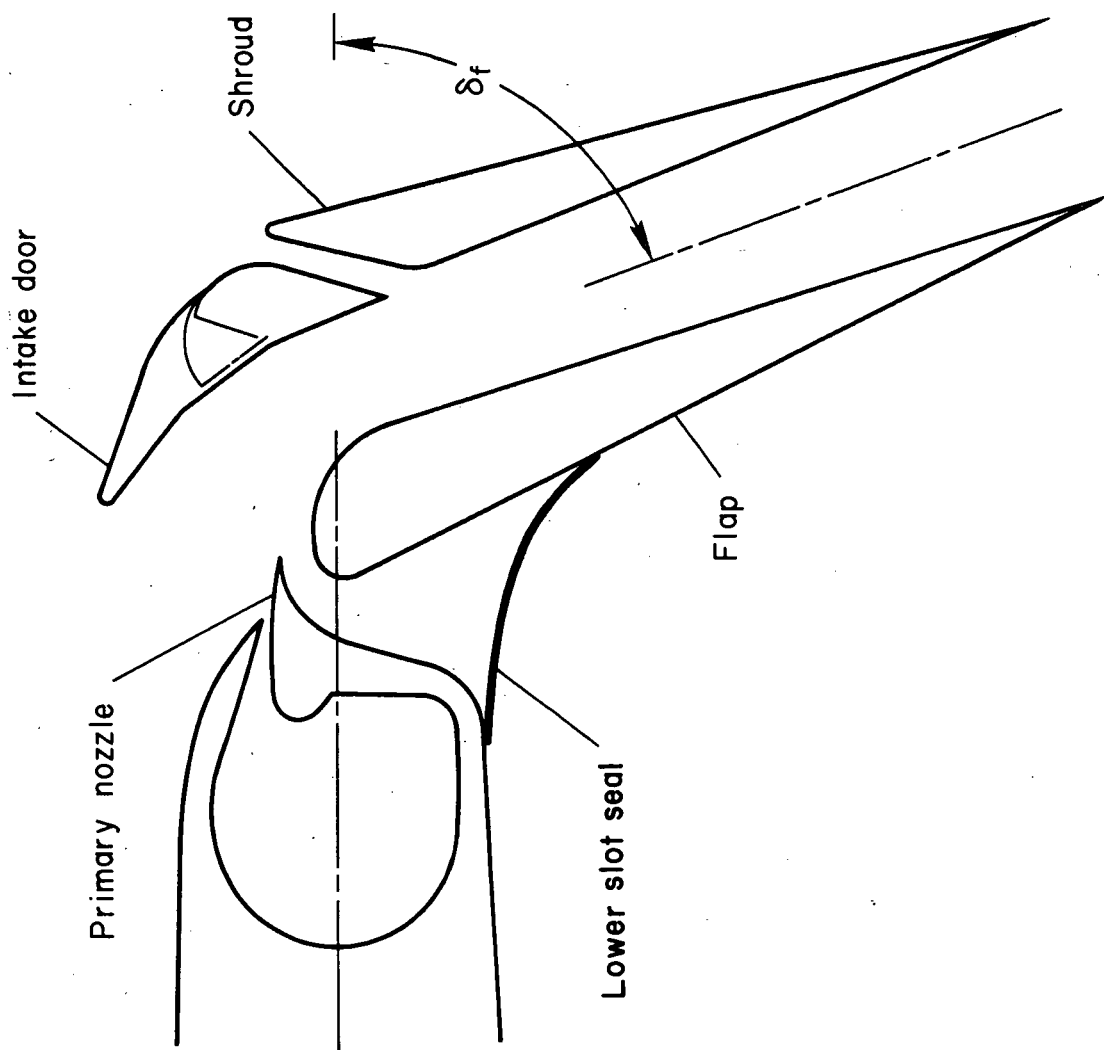
Figure 6.— Sealing of augmentor lower slot.

Shroud

Intake door

Primary nozzle

δ_f

Flap

Lower slot seal
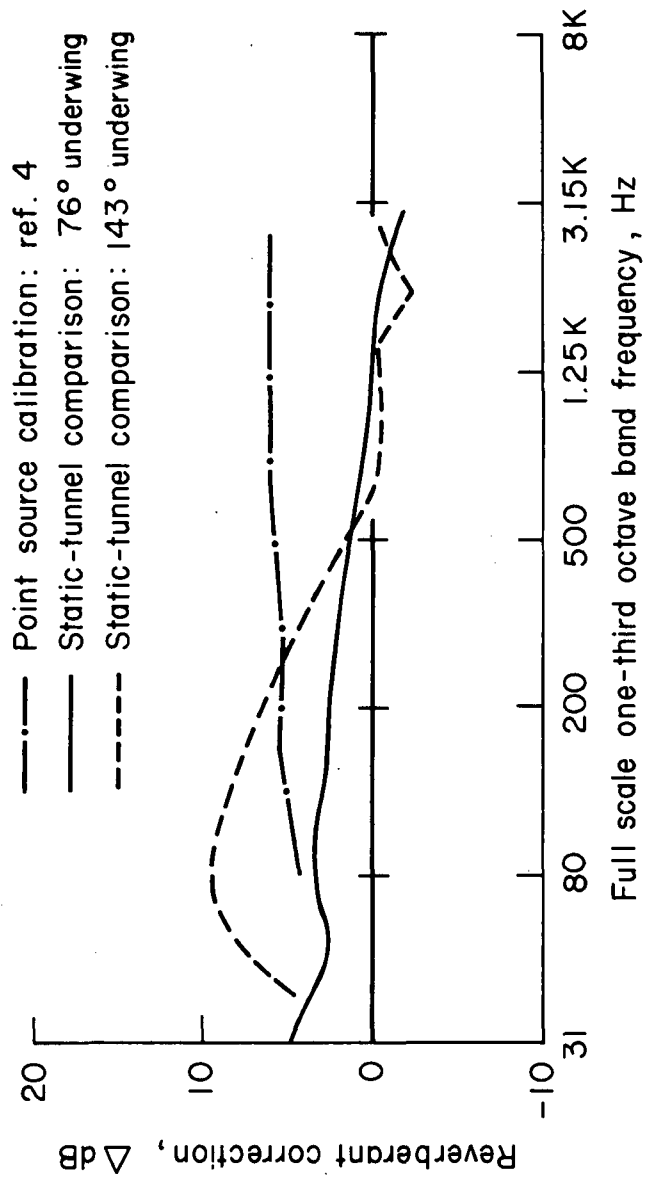
Figure 7.— Wind tunnel test section reverberation.
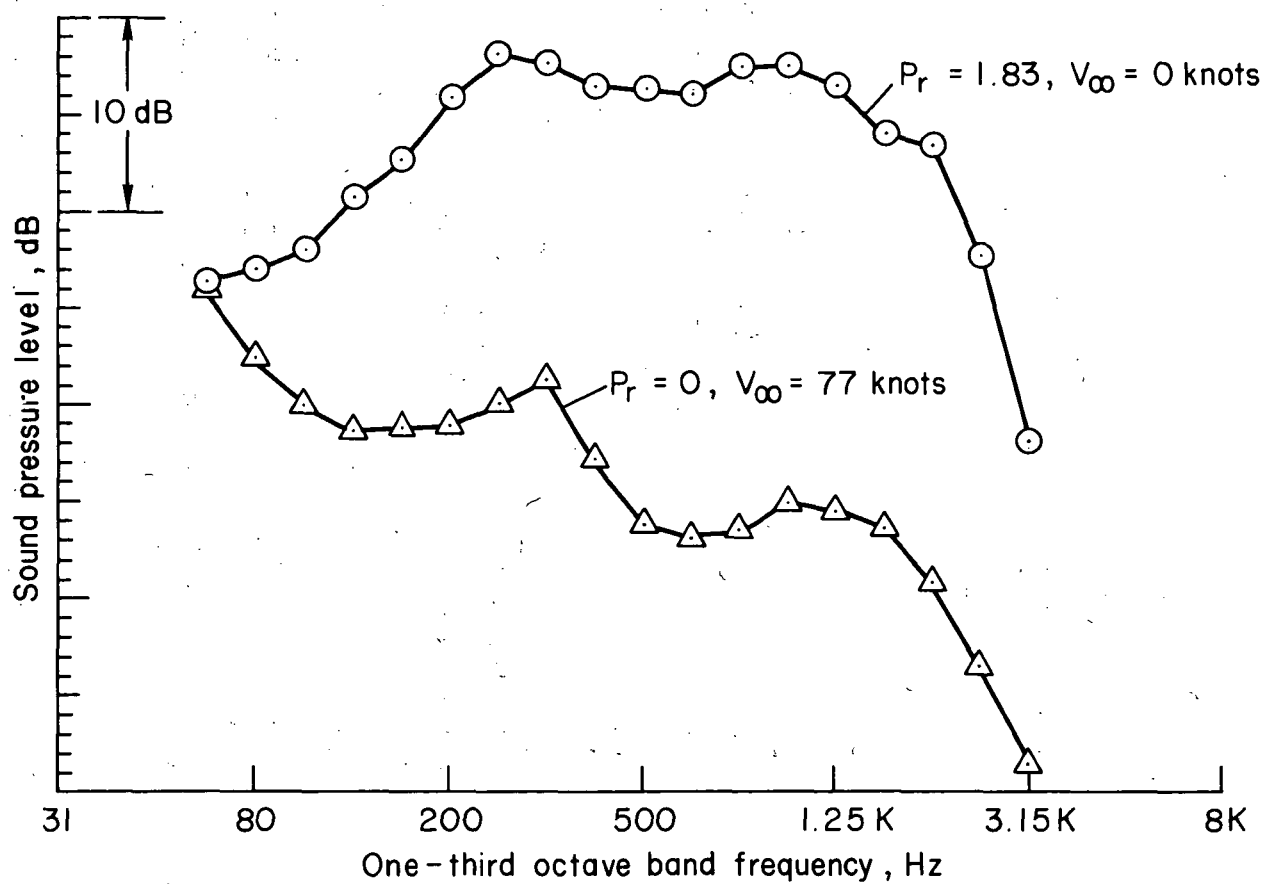
Figure 8.— Wind tunnel test section background noise floor. Underwing mic. azimuth = 97°.
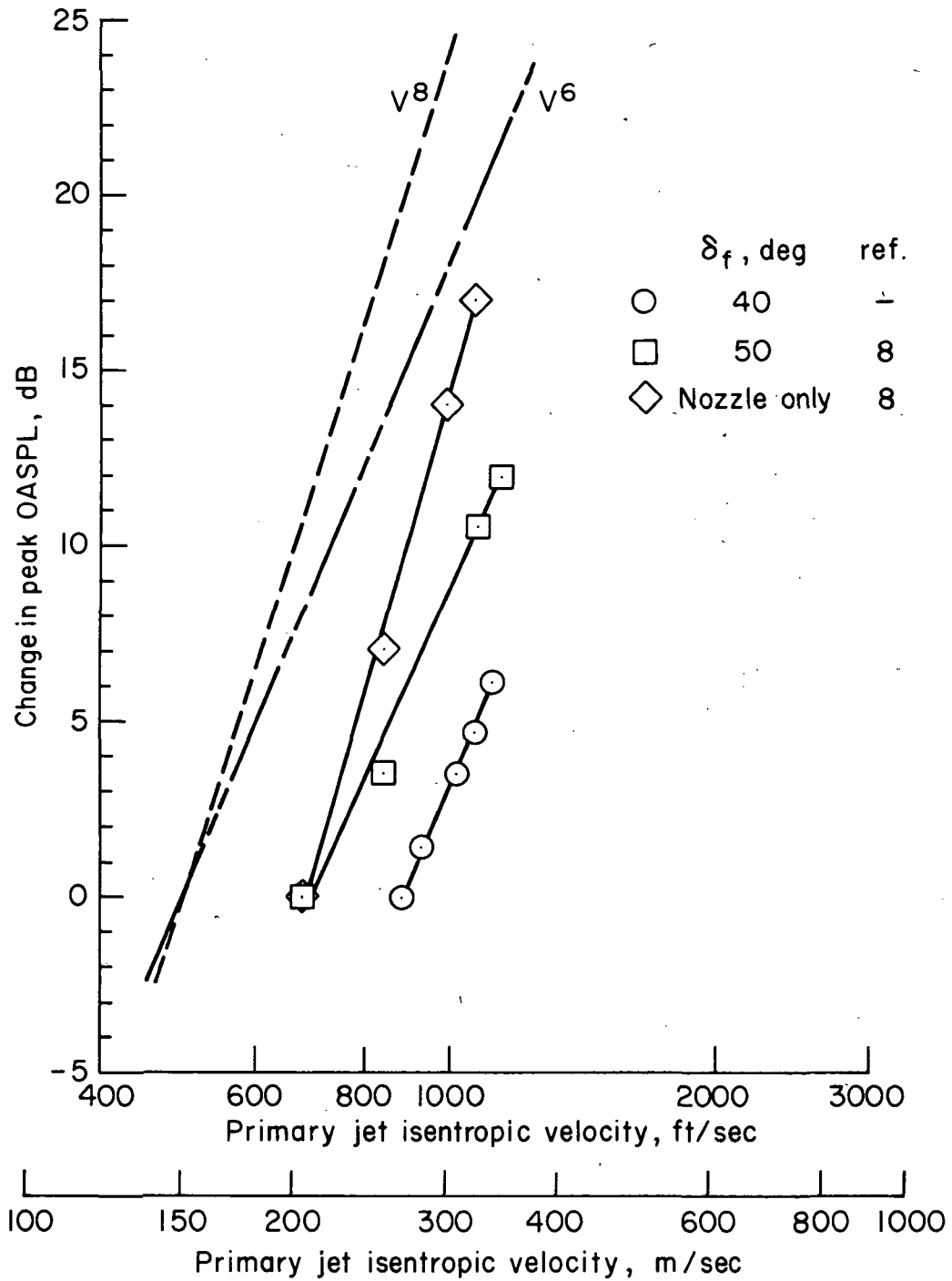
Figure 9.— Effect of primary jet velocity on augmentor acoustics. $V_\infty = 0$ knots.
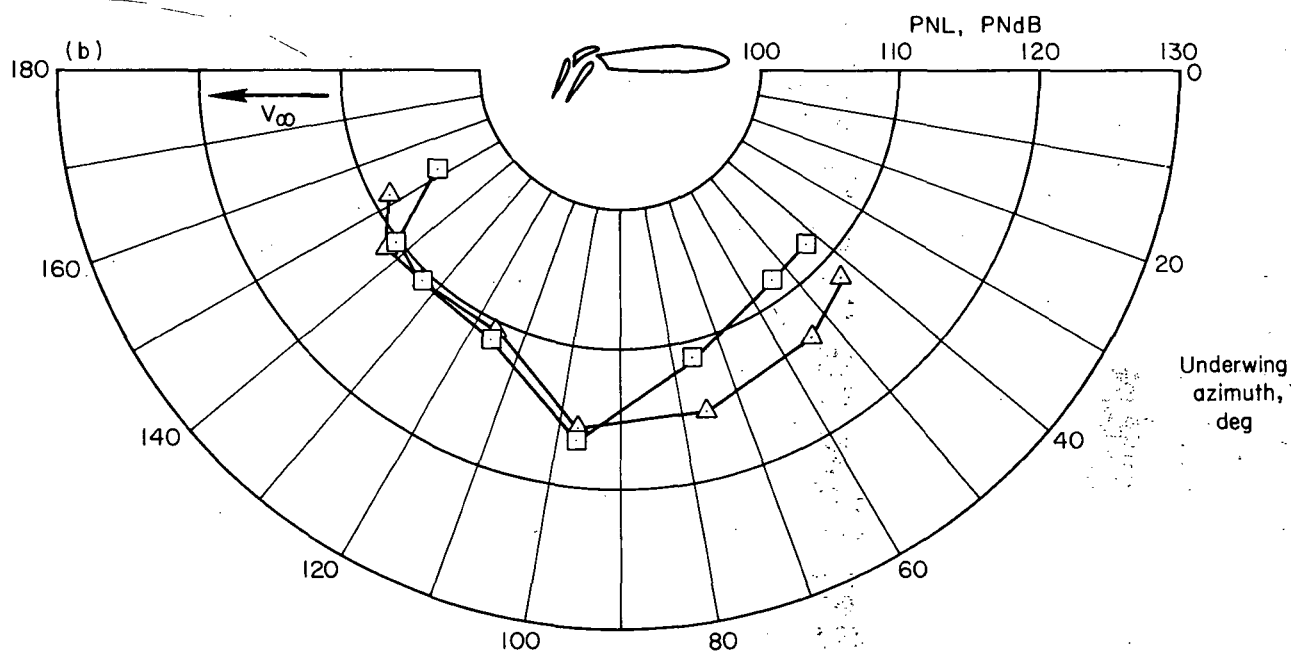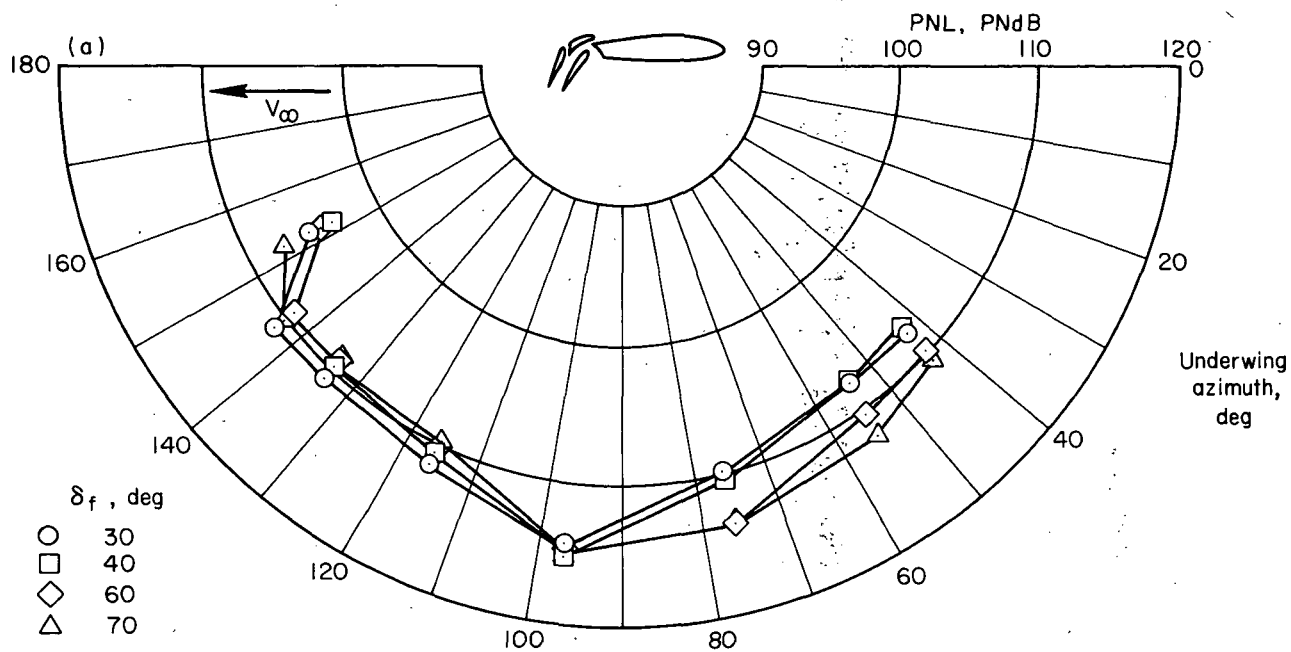
(a) $P_r = 1.83$

(b) $P_r = 1.91$

Figure 10.— Variation of underwing PNL directivity patterns with flap deflection. $V_\infty = 0$ knots.
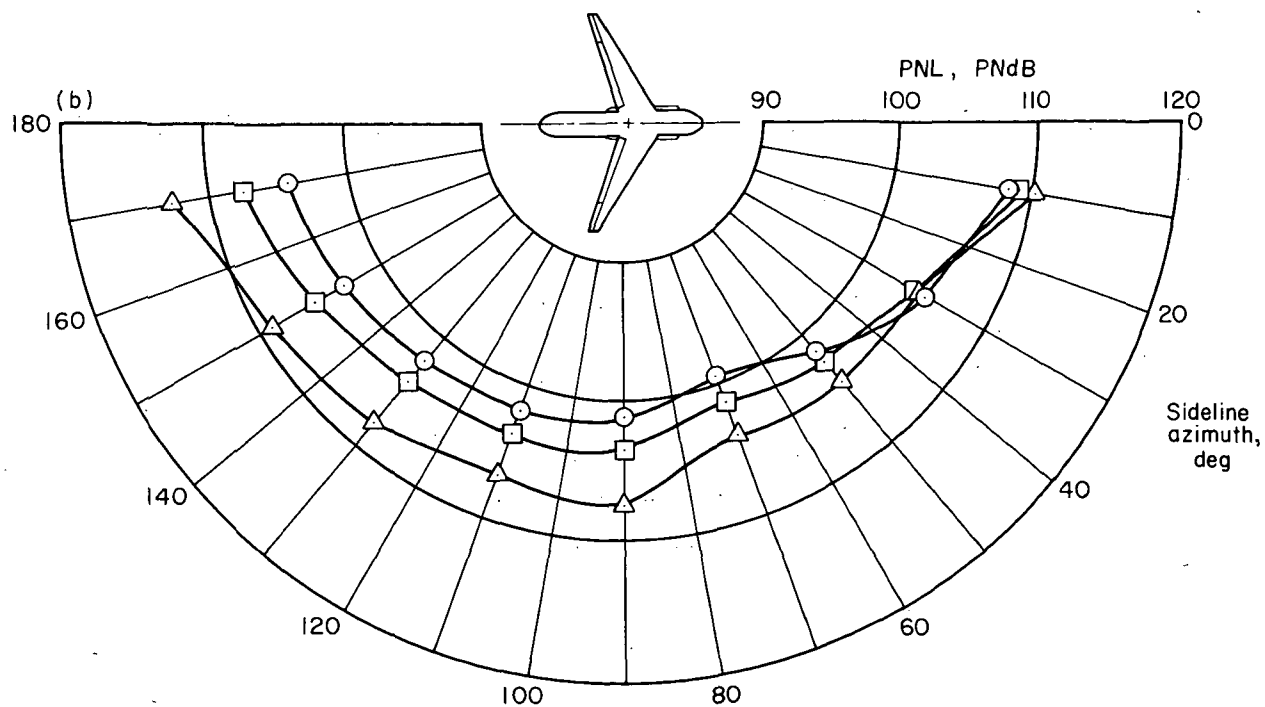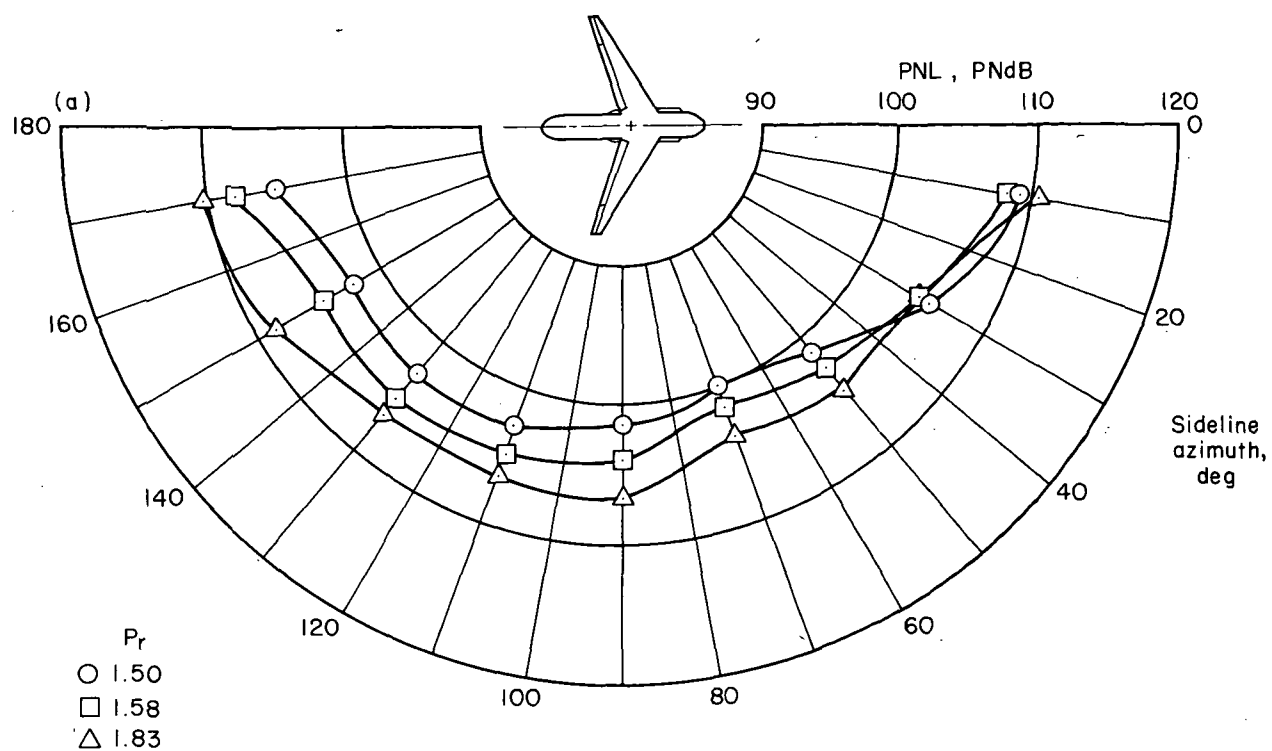
(a) $\delta_f = 40°$

(b) $\delta_f = 50°$

Figure 11.— Sideline perceived noise level directivity patterns for several flap deflections.
$V_\infty = 0$ knots
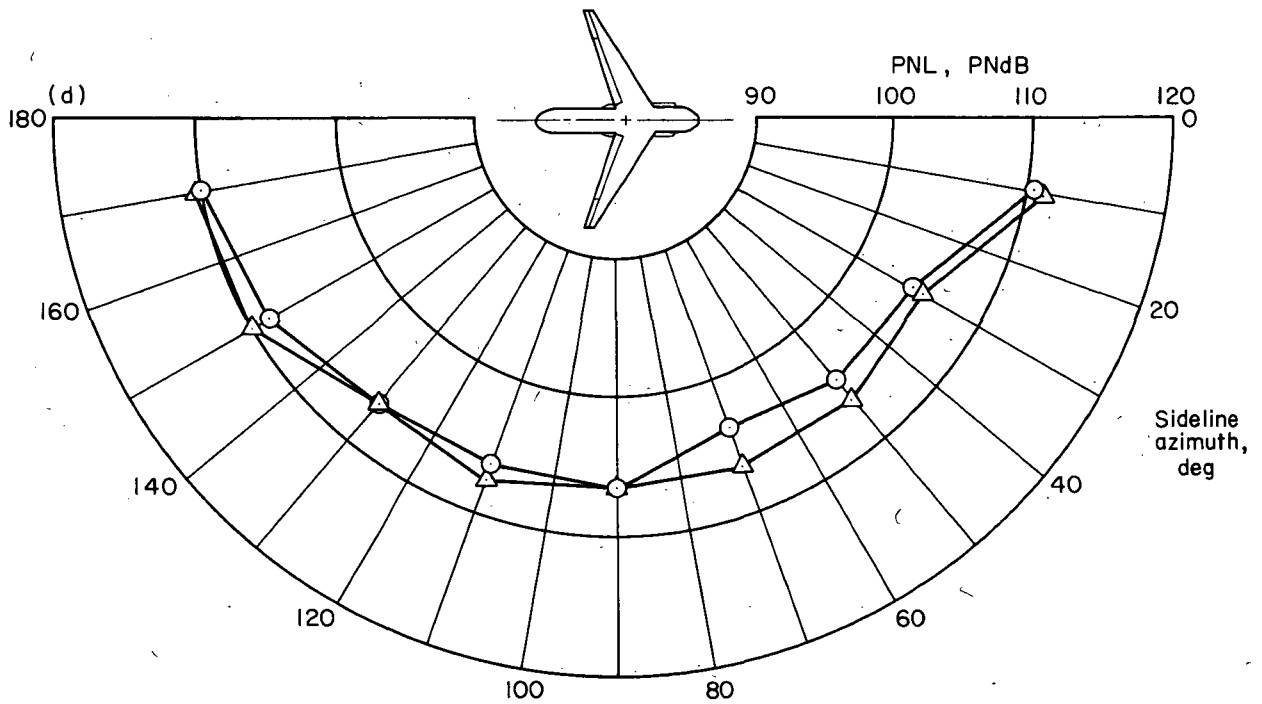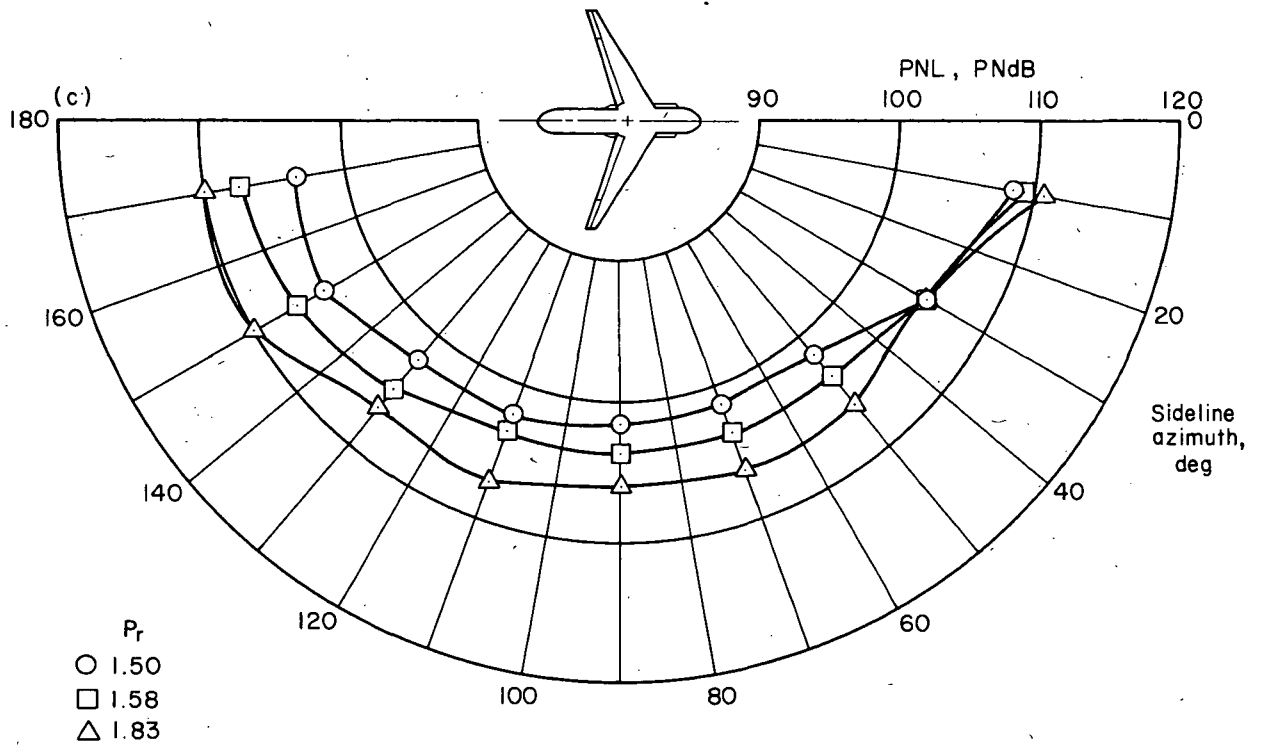
(c) $\delta_f = 70°$

(d) $\delta_f = 40°$ and $70°$, $P_r = 1.83$

Figure 11.— Concluded.
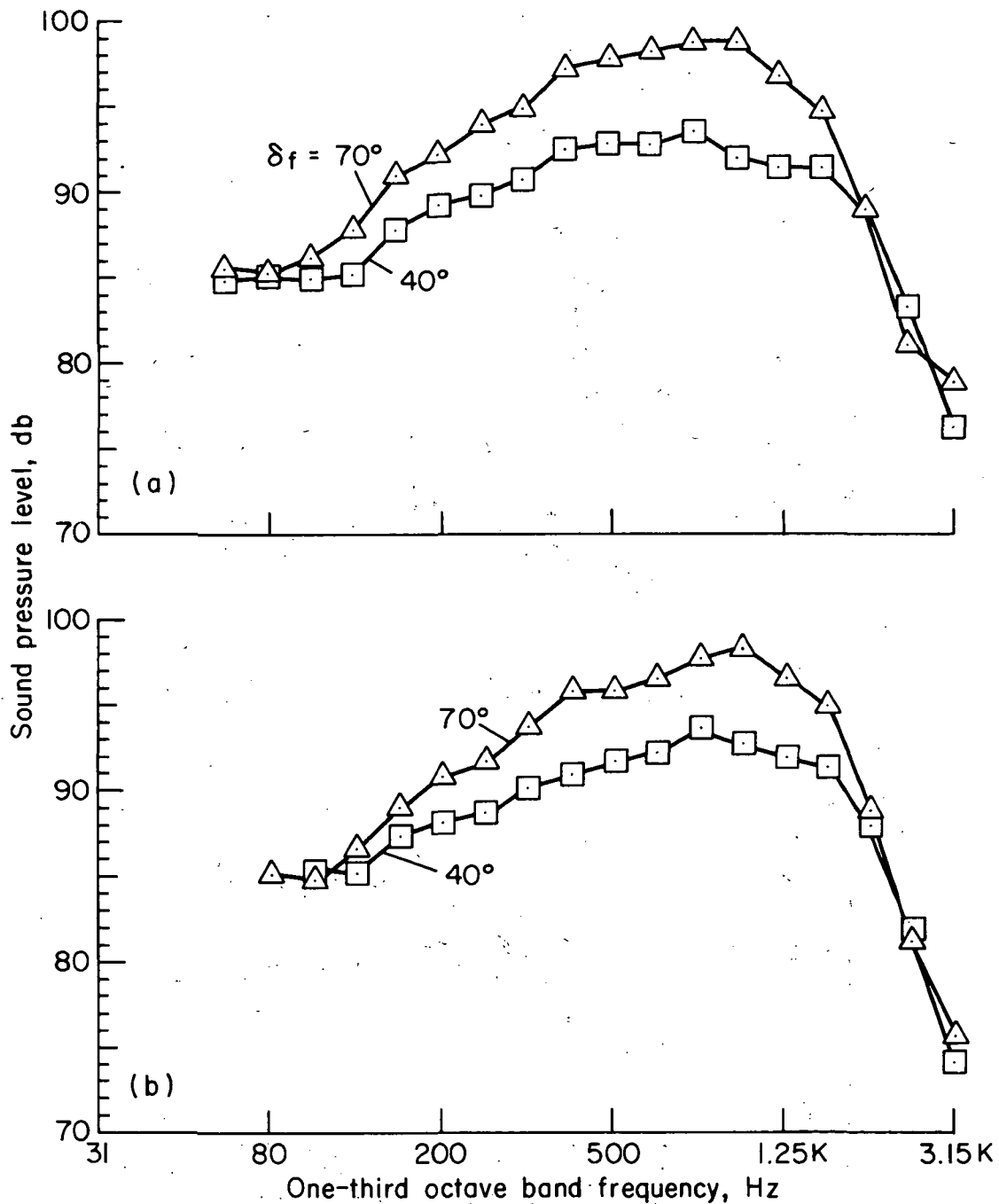
(a) $V_\infty = 0$ knots.

(b) $V_\infty = 77$ knots.

Figure 12.— Variation of sound frequency spectra with flap deflection. $P_r = 1.83$; underwing mic. azimuth = 76°.

(a) $V_\infty = 0$ knots.

(b) $V_\infty = 39$ knots.
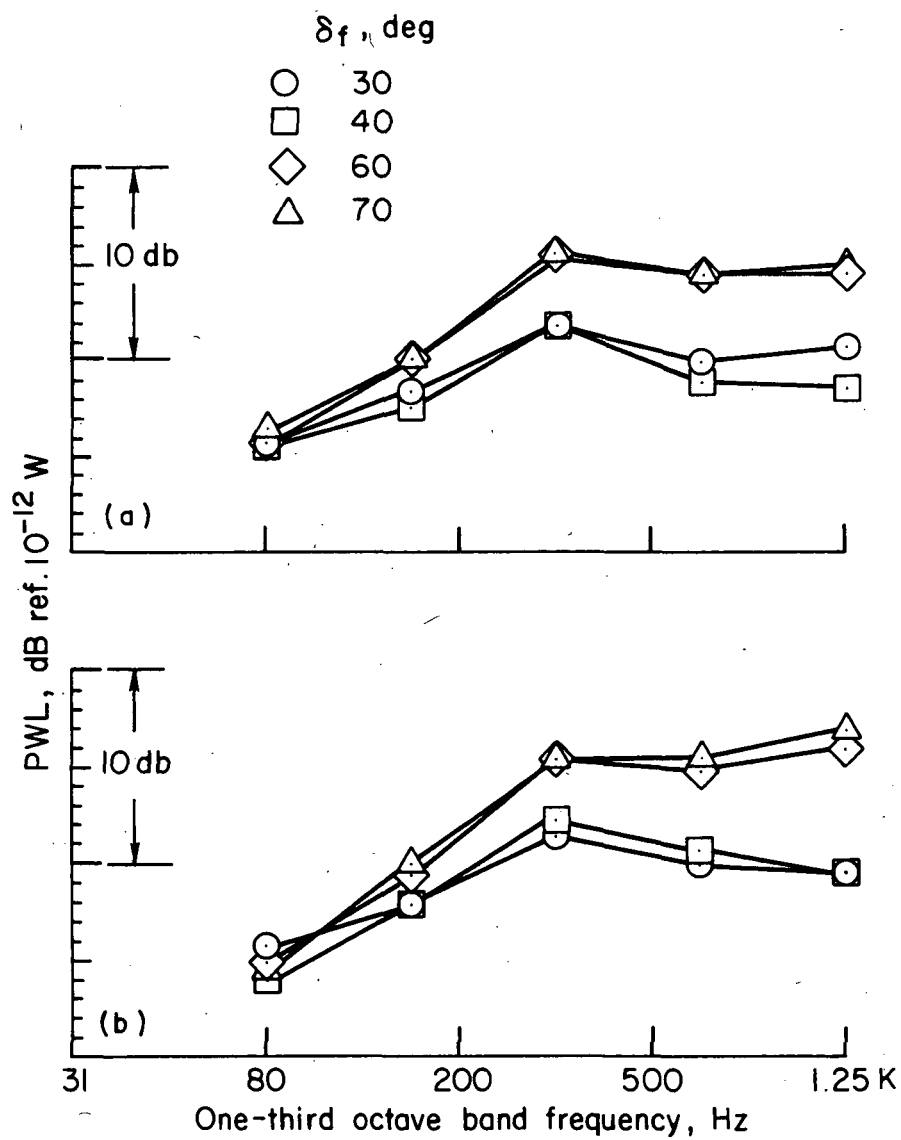
Figure 13.— Effect of flap deflection on acoustic sound power level. $P_r = 1.83$.
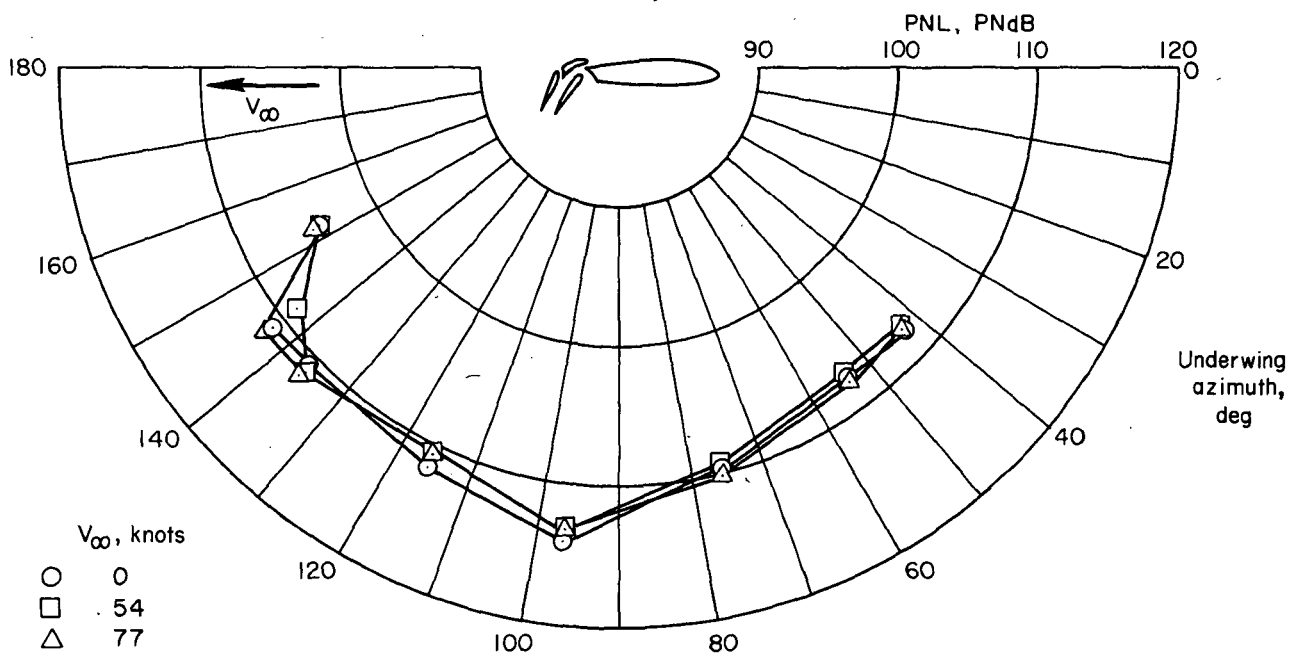
Figure 14.— Variation of PNL directivity with free-stream velocity. $\delta_f = 30$; $P_r = 1.83$.
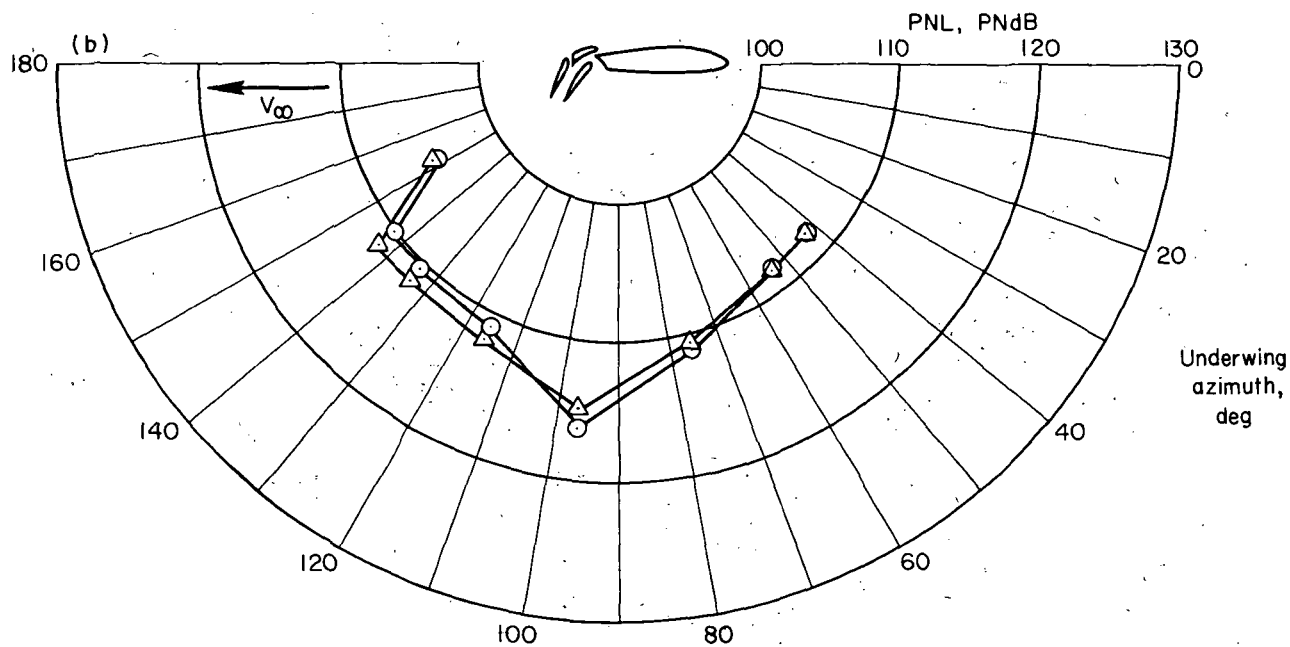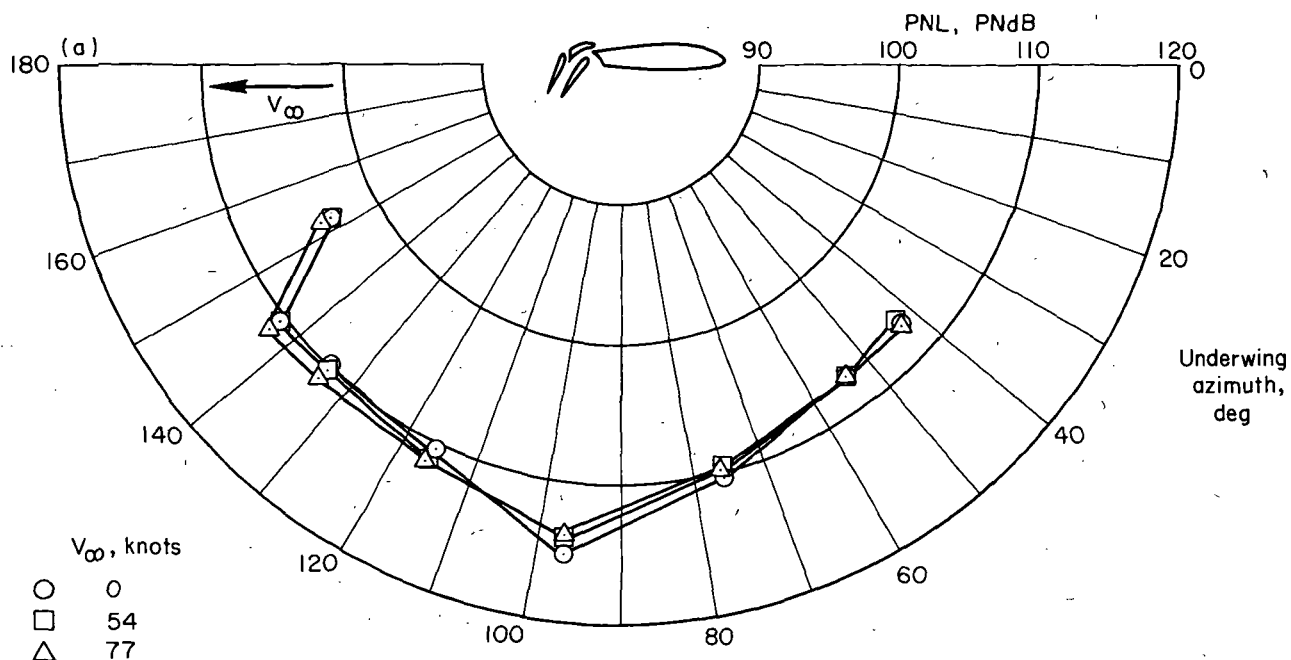
(a) $P_r = 1.83$

(b) $P_r = 1.91$

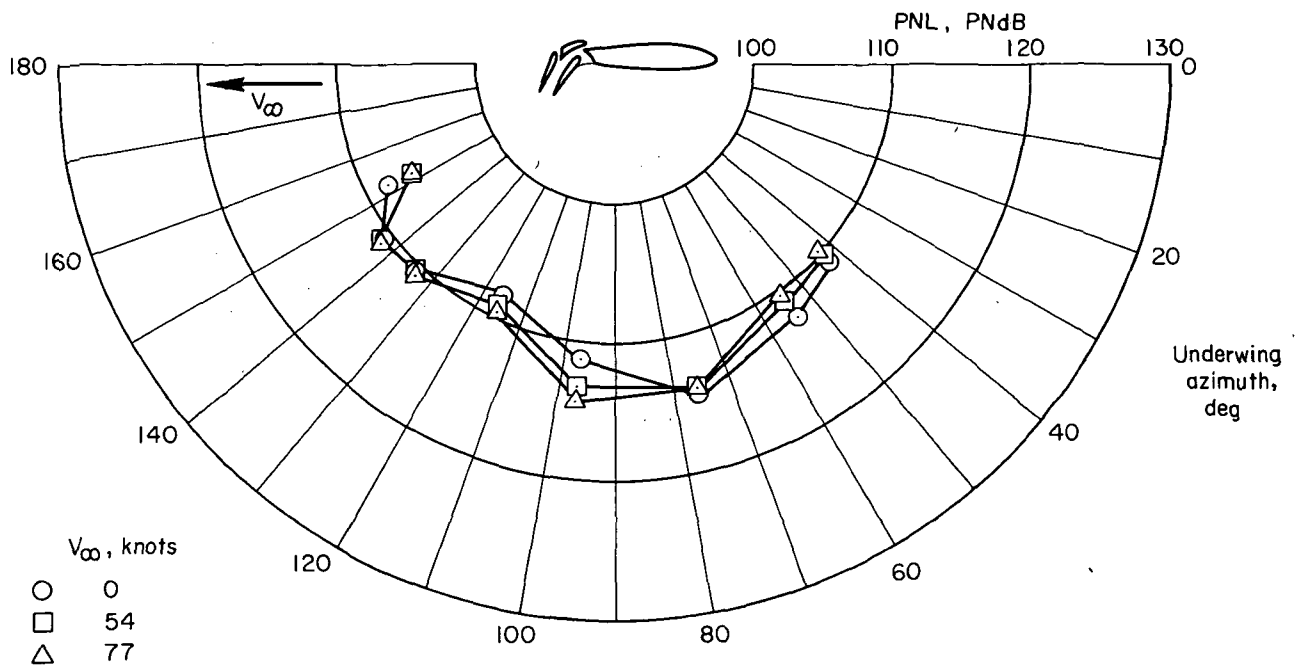Figure 15.— Variation of PNL directivity with free-stream velocity. $\delta_f = 40°$.
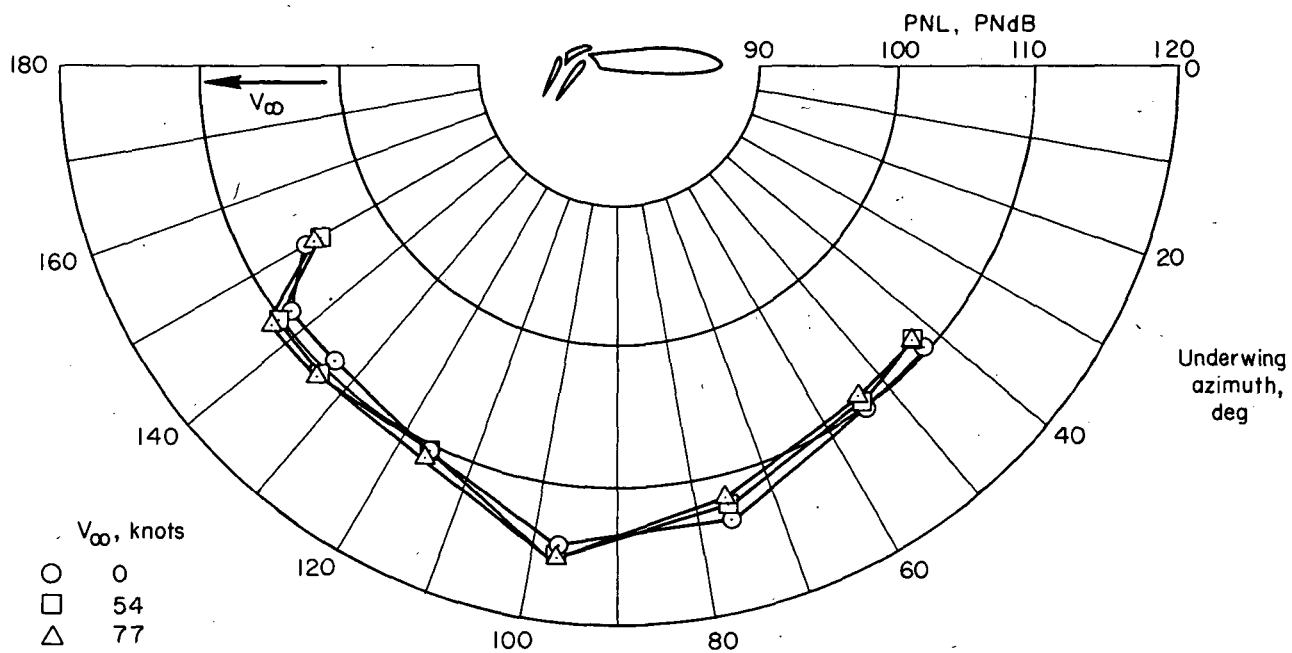
Figure 16.— Variation of PNL directivity with free-stream velocity. $\delta_f = 60°$; $P_r = 1.83$.
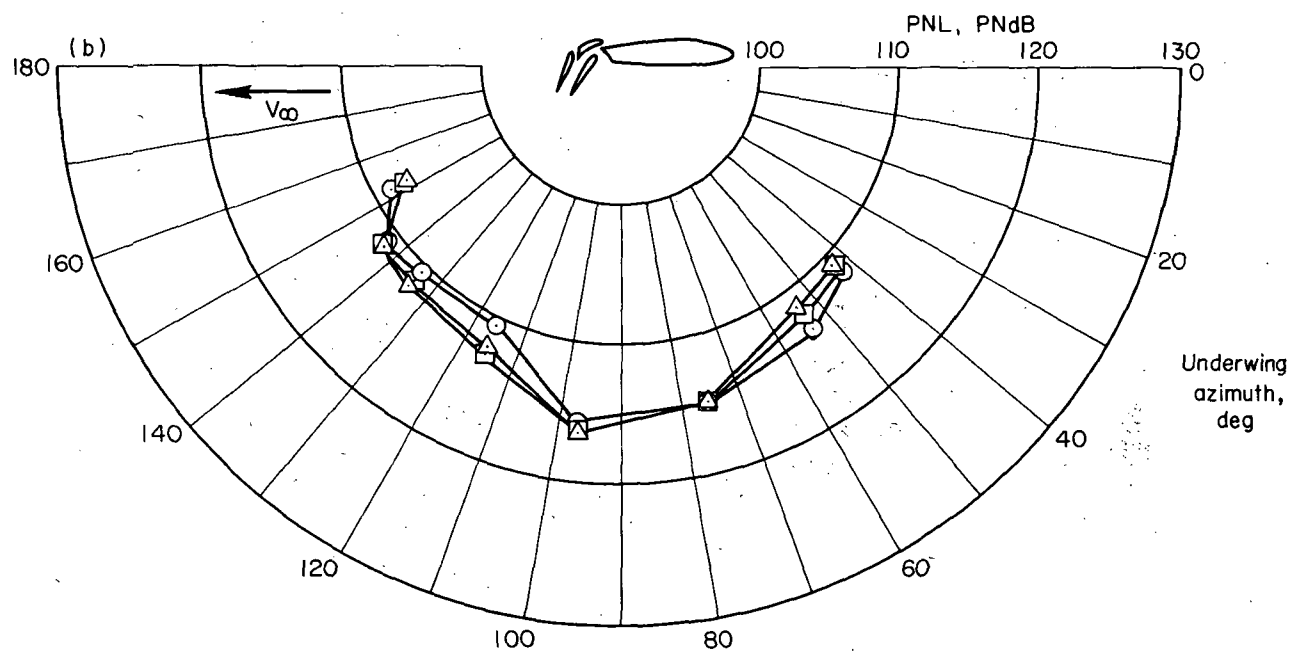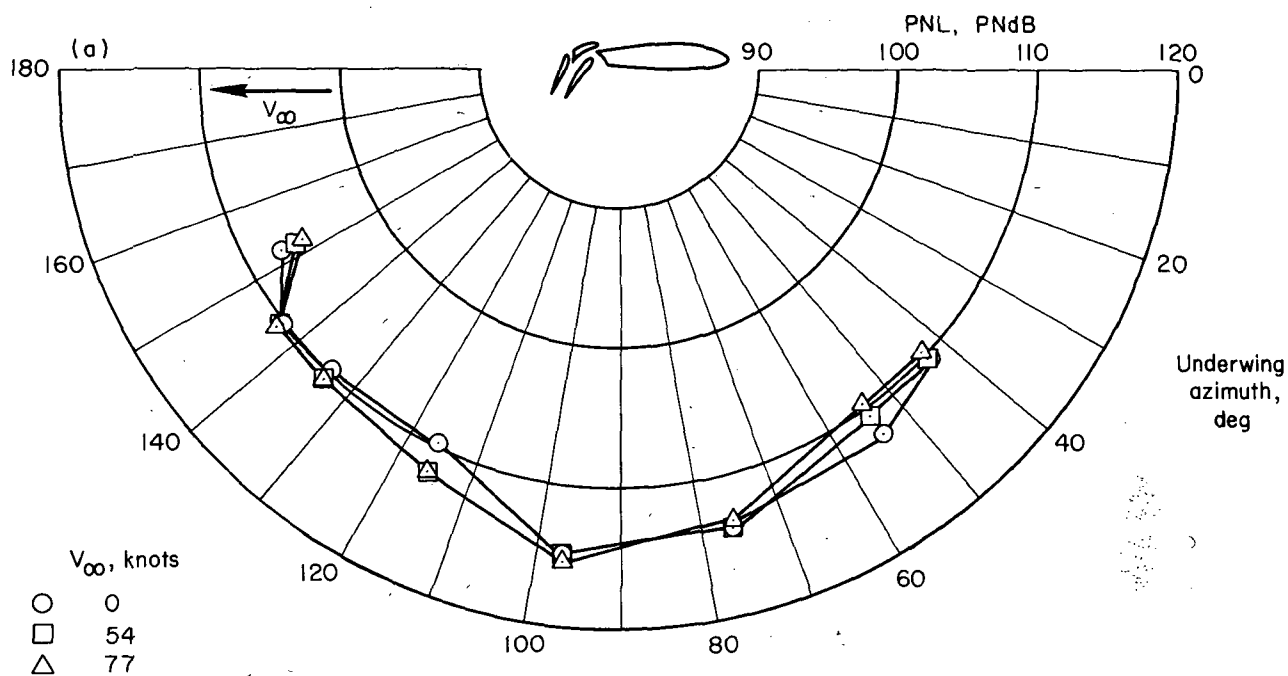
(a) $P_r = 1.83$

(b) $P_r = 1.91$

Figure 17.— Variation in PNL directivity with free-stream velocity. $\delta_f = 70°$.

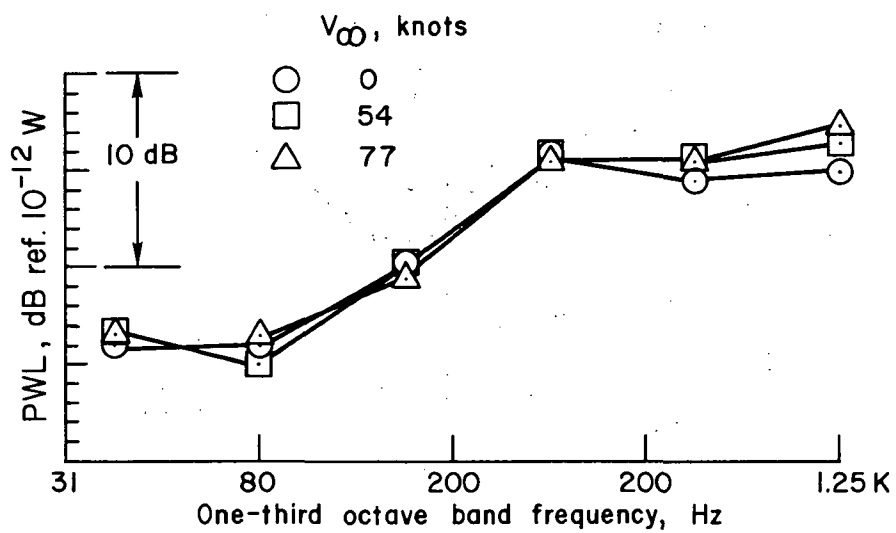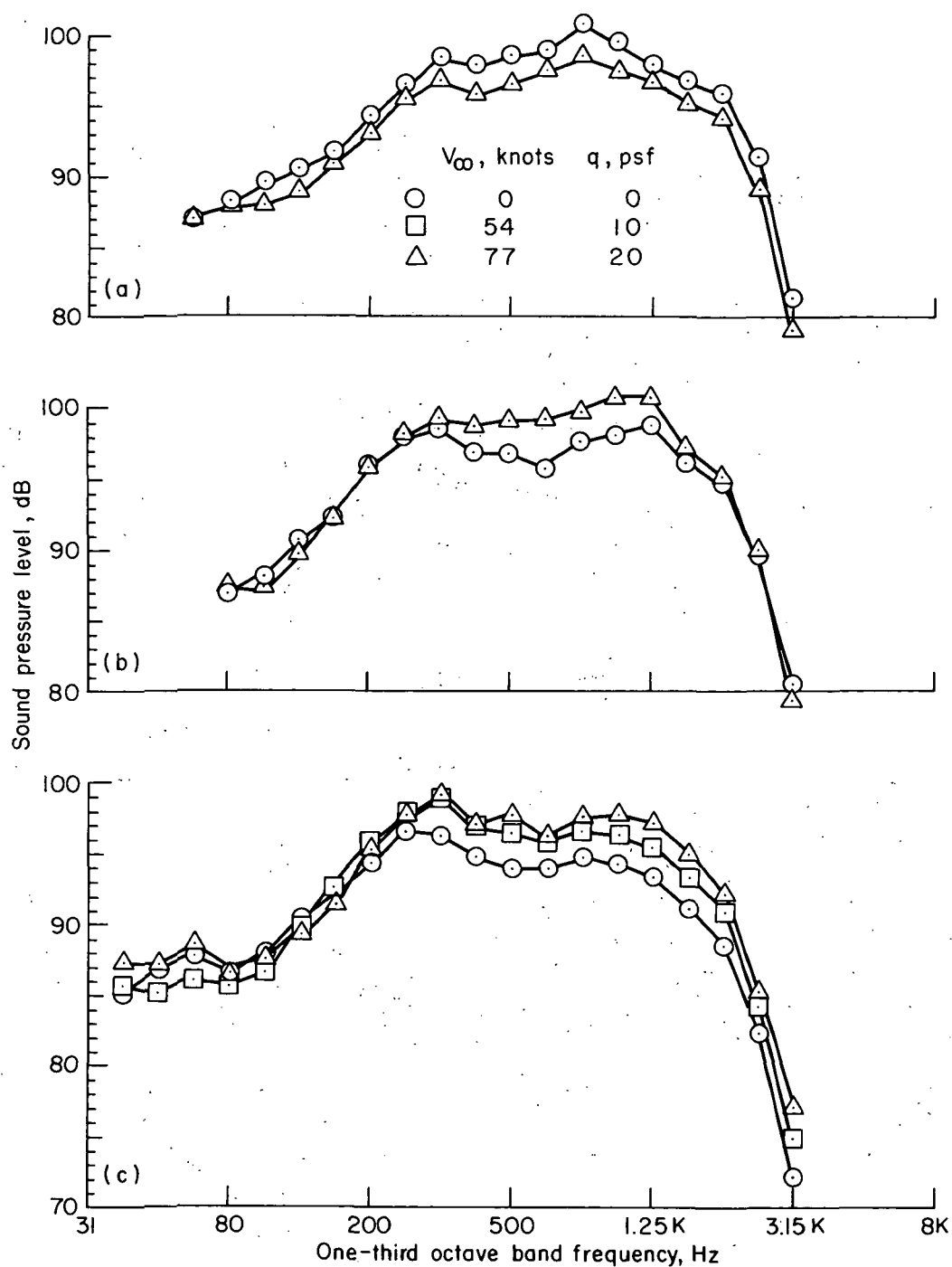Figure 18.— Variation in PNL directivity with free-stream velocity. $\delta_f = 70°$; lower slot sealed; $P_r = 1.83$.

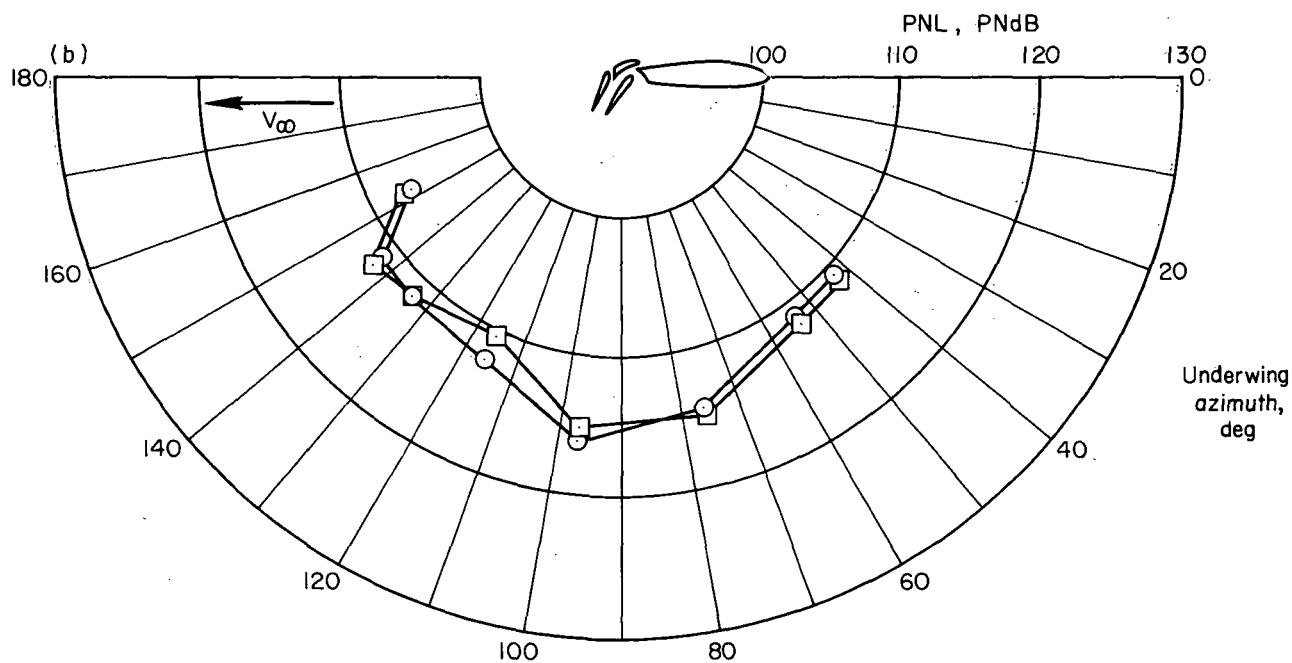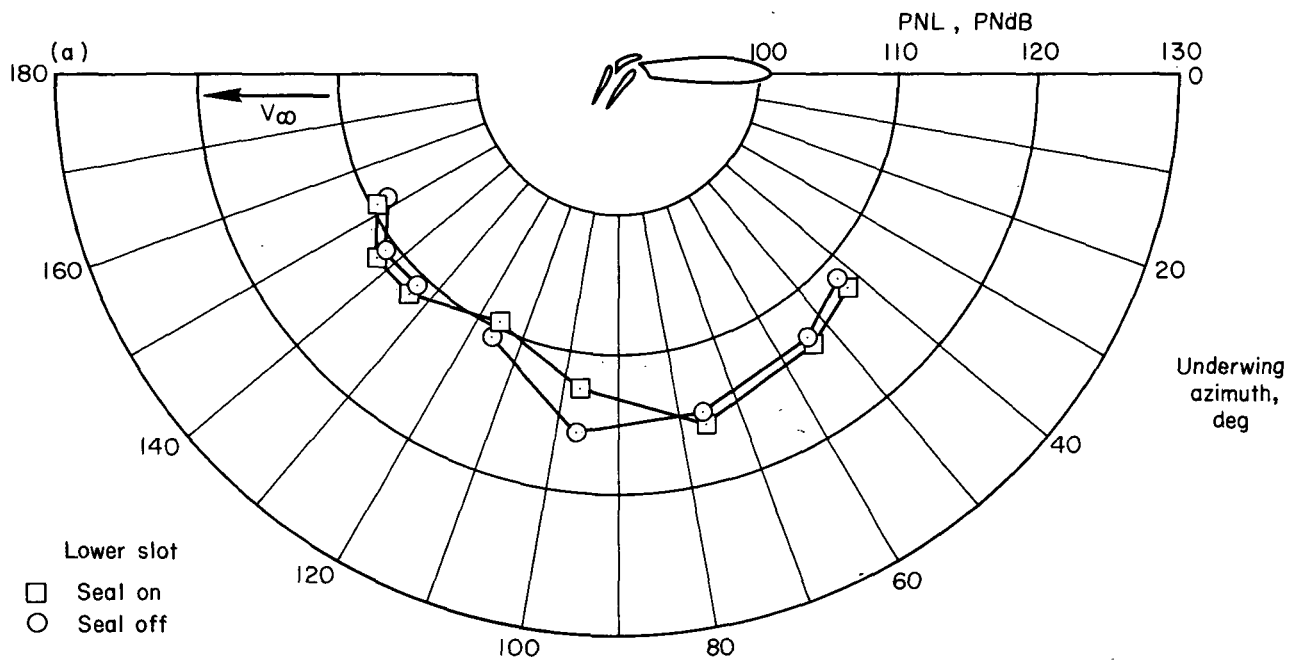Figure 19.— Effect of free-stream velocity on sound power level. $\delta_f = 70°$; $P_r = 1.83$.

(a) $\delta_f = 40°$ and $P_r = 1.91$.

(b) $\delta_f = 70°$ and $P_r = 1.91$.

(c) $\delta_f = 70°$; $P_r = 1.83$; and lower slot sealed.

Figure 20.— Variation of frequency spectrum with free-stream velocity.
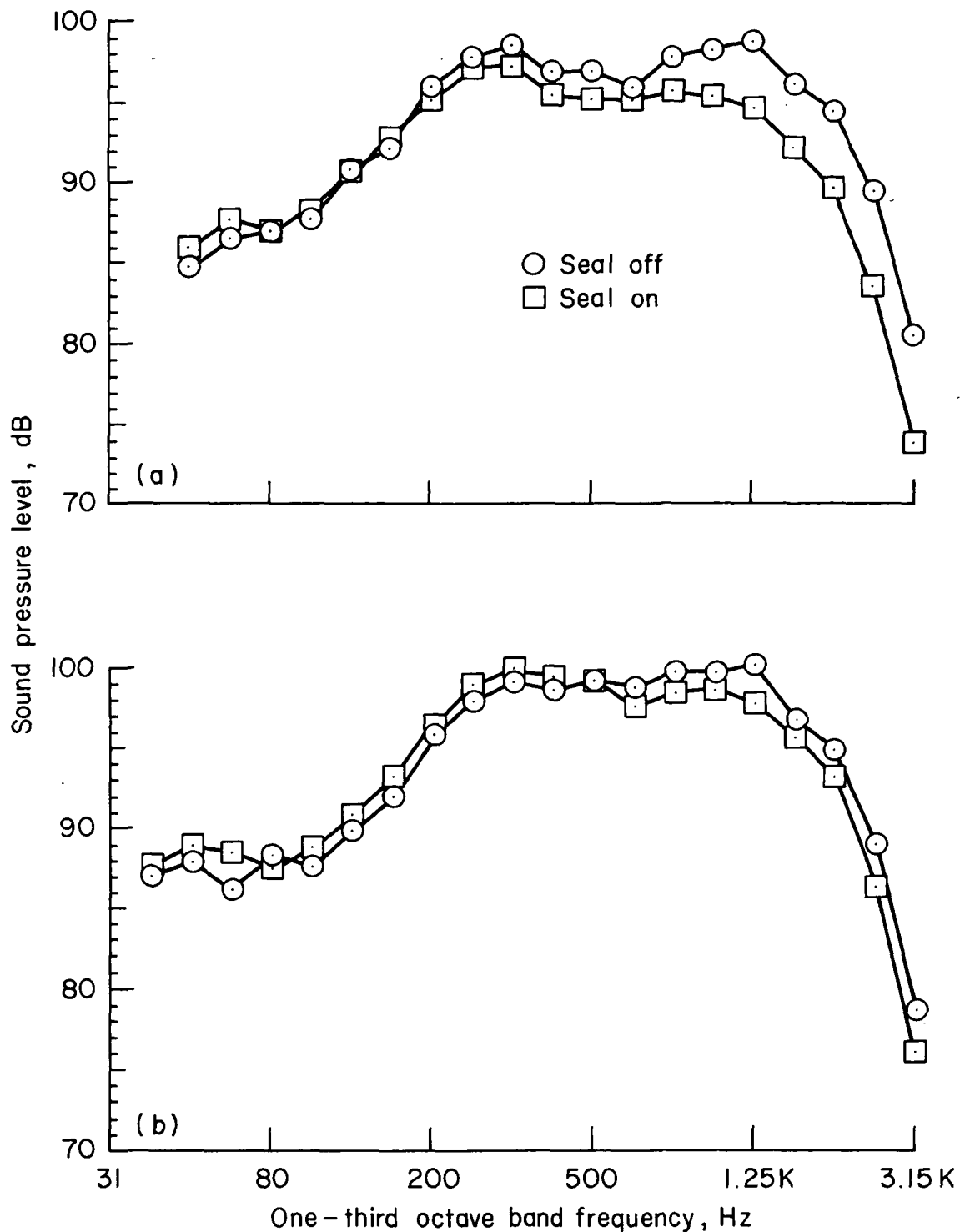Underwing mic. azimuth = 97°.

(a) $V_\infty = 0$ knots.

(b) $V_\infty = 77$ knots.

Figure 21.— Effect of lower slot seal on PNL directivity pattern. $\delta_f = 70°$; $P_r = 1.91$.

(a) $V_\infty = 0$ knots.

(b) $V_\infty = 77$ knots.

Figure 22.— Effect of lower slot seal on the frequency spectrum. $\delta_f = 70°$; $P_r = 1.91$; under wing mic. azimuth $= 97°$.

*"The aeronautical and space activities of the United States shall be
conducted so as to contribute . . . to the expansion of human knowl-
edge of phenomena in the atmosphere and space. The Administration
shall provide for the widest practicable and appropriate dissemination
of information concerning its activities and the results thereof."*
—NATIONAL AERONAUTICS AND SPACE ACT OF 1958

NASA SCIENTIFIC AND TECHNICAL PUBLICATIONS

TECHNICAL REPORTS: Scientific and
technical information considered important,
complete, and a lasting contribution to existing
knowledge.

TECHNICAL NOTES: Information less broad
in scope but nevertheless of importance as a
contribution to existing knowledge.

TECHNICAL MEMORANDUMS:
Information receiving limited distribution
because of preliminary data, security classifica-
tion, or other reasons. Also includes conference
proceedings with either limited or unlimited
distribution.

CONTRACTOR REPORTS: Scientific and
technical information generated under a NASA
contract or grant and considered an important
contribution to existing knowledge.

TECHNICAL TRANSLATIONS: Information
published in a foreign language considered
to merit NASA distribution in English.

SPECIAL PUBLICATIONS: Information
derived from or of value to NASA activities.
Publications include final reports of major
projects, monographs, data compilations,
handbooks, sourcebooks, and special
bibliographies.

TECHNOLOGY UTILIZATION
PUBLICATIONS: Information on technology
used by NASA that may be of particular
interest in commercial and other non-aerospace
applications. Publications include Tech Briefs,
Technology Utilization Reports and
Technology Surveys.

Details on the availability of these publications may be obtained from:

SCIENTIFIC AND TECHNICAL INFORMATION OFFICE

NATIONAL AERONAUTICS AND SPACE ADMINISTRATION
Washington, D.C. 20546